

國立臺灣大學工學院化學工程研究所



碩士論文

Graduate Institute of Chemical Engineering

College of Engineering

National Taiwan University

Master Thesis

利用液態氫源與雙功能鈀鈷的碳球在常溫常壓下製備

2,5-二甲基呋喃

Novel Synthesis of 2,5-Dimethylfuran under Ambient Conditions

Utilizing ZIF-67 Derived Bifunctional Carbon Supported

Palladium and Cobalt with Aqueous Hydrogen Source

吳霈恩

Pei-En Wu

指導教授：吳嘉文 博士

Advisor: Kevin Chia-Wen Wu, Ph.D.

中華民國 103 年 7 月

July, 2014

國立臺灣大學碩士學位論文
口試委員會審定書

利用液態氫源與雙功能鈀鈷的碳球在常溫常壓下製備
2,5-二甲基呋喃

Novel Synthesis of 2,5-Dimethylfuran under Ambient
Conditions Utilizing ZIF-67 Derived Bifunctional Carbon
Supported Palladium and Cobalt with Aqueous Hydrogen
Source

本論文係吳霈恩君 (R01524095) 在國立臺灣大學化學工程學系、
所完成之碩士學位論文，於民國 103 年 07 月 01 日承下列考試委員審
查通過及口試及格，特此證明

口試委員：

吳 嘉 文

(簽名)

(指導教授)

橫井 俊之

橫井 俊之

小林 広和

小林 広和

中島 清隆

中島 清隆

多湖 輝興

多湖 輝興

王大銘

(簽名)

系主任、所長

(是否須簽章依各院系所規定)

誌謝



此研究論文能順利完成，首先要感謝我的指導老師吳嘉文在這兩年的時間時常與我討論實驗及提供給我這個題目，此外也感謝老師給予我完整的訓練，在實驗室的維護還有與廠商的溝通也都讓我有許多的學習。再來要感謝學姊徐韶徽為這項研究貢獻了許多的想法還有方向讓這項研究能順利完成，在這過程讓我對於實驗的構想有新的學習與成長。

我也要感謝實驗室的各位陪伴我度過在實驗室的這兩年：感謝毓璞和瑜婷常常提醒我關於一些行政的事項。感謝靖天跟我討論實驗，好讓我可以得到改進實驗的想法。感謝有衡為我測量了許多材料的鑑定。感謝亨達在材料製備上的測試。最後我要感謝大家一起維護實驗室的環境，好讓我們可以有一個共同可以完成研究的空間。

ABSTRACT



The ever increasing demand for energy combined with the diminishing supply of fossil fuel signals the need to search for an alternative energy source. 2,5-Dimethylfuran (DMF) is a green and renewable fuel due to its lignocellulosic origin. The production of DMF results from the hydrogenation and hydrogenolysis of 5-Hydroxymethylfurfural (HMF). Hydrogenation processes often require purging the system with high pressure hydrogen to increase the solubility of hydrogen in the solvent, all the while using high temperatures for the hydrogenation reactions to occur. Herein, we proposed a novel method in which DMF could be synthesized in high yields under atmospheric pressure and room temperature.

A bifunctional Pd/CoNC material of ZIF-67 descent was synthesized in which Palladium provides a hydrogenation surface and Cobalt catalyzes the production of hydrogen from an aqueous source, Sodium Borohydride (NaBH_4). The synergetic effects of Cobalt and Palladium on the same support helped achieve 83.07% DMF yields.

Keywords: Biomass, 2,5-Dimethylfuran, ZIF-67, hydrogenation, bifunctional.

摘要



由於能源的需求越來越大，加上石油的供應終將面臨短缺，有再生能力並且環保的生質能源因此受到矚目。其中，由木質纖維素所製備的 2,5-二甲基咪喃因性質接近汽油，因此可取代汽油或成為汽油添加物。藉由氫化可以將 5-甲基糠醛轉換成 2,5-二甲基咪喃。氫化反應大多需要高溫達成活化能與通入高壓氫氣提高氫氣於溶劑中的溶解值。在此，我們提供一反應系統在室溫與室壓下即能製備 2,5-二甲基咪喃。

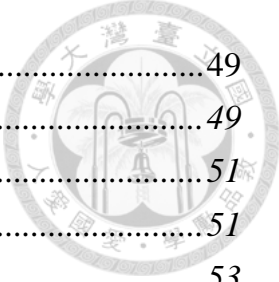
此實驗由 ZIF-67(Zeolitic Imidazolate Framework)合成的雙功能鈰鈷奈米孔洞碳材，鈰能提供氫化反應所需的金屬表面並利用鈷催化氫硼化鈉可於液態產氫。鈰與鈷在同一材料上的協同作用使得我們可以在室溫與室壓下得到 83.07% 產率的 2,5-二甲基咪喃。

關鍵字：生質能源、2,5-二甲基咪喃、ZIF-67、氫化反應、雙官能化

TABLE OF CONENTS



1. INTRODUCTION.....	1
1.1. ENERGY CRISIS.....	1
1.2. BIOMASS DEVELOPMENT.....	4
1.3. BIOMASS CONVERSION	6
2. PAPER SURVEY	9
2.1. METAL ORGANIC FRAMEWORK (MOF) BASED CATALYSTS	9
2.2. INCIPIENT WETNESS IMPREGNATION ³⁷	11
2.3. PRODUCTION OF 2,5-DIMETHYLFURAN.....	15
3. OBJECTIVE.....	20
4. EXPERIMENTAL	22
4.1. CHEMICALS AND MATERIALS.....	22
4.2. EQUIPMENT	23
4.3. PROCEDURE FOR PRODUCTION OF 2,5-DIMETHYLFURAN	24
4.3.1. <i>Batch Reactions</i>	24
4.3.2. <i>Semi-Batch Reactions</i>	26
4.4. CATALYST SYNTHESIS	28
4.4.1. <i>ZIF-67 Synthesis</i>	28
4.4.2. <i>ZIF-67 to Pd/CoNC Conversion</i>	30
4.5. CHARACTERIZATION.....	31
4.5.1. <i>Scanning Electron Microscope (SEM)</i>	31
4.5.2. <i>Transmission electron microscopy (TEM)</i>	37
4.5.3. <i>Specific Surface Area Analyzer</i>	42
4.5.4. <i>X-Ray Diffraction (XRD)</i>	44
4.5.5. <i>Thermogravimetric Analysis</i>	46
4.5.6. <i>Calibration Curve for DMF</i>	48
4.5.7. <i>Calibration Curve for MFAD</i>	48
5. RESULTS AND DISCUSSION.....	49



5.1.	HMF AS THE STARTING REACTANT.....	49
5.1.1.	<i>Effect of Catalyst Amount</i>	49
5.1.2.	<i>Effect of Reaction Temperature</i>	51
5.1.3.	<i>Effect of Reaction Time</i>	51
5.1.4.	<i>Effect of NaOH addition</i>	53
5.2.	COMPARISON OF DIFFERENT STARTING REACTANTS	55
5.3.	PALLADIUM AND COBALT ON SAME OR DIFFERENT SUPPORTS.....	57
5.4.	REACTIONS STARTING WITH MFAD.....	58
5.4.1.	<i>With or Without Acid Addition</i>	58
5.5.	DIFFERENT STARTING REACTANTS UNDER OPTIMUM CONDITIONS.....	62
5.6.	EFFECT OF ATM OR NON-ATM PRESSURE TESTS	63
5.7.	SYNERGETIC EFFECTS OF COBALT AND PALLADIUM.....	64
6.	CONCLUSION.....	66
7.	FUTURE PROSPECTS.....	67
8.	REFERENCE.....	69

LIST of FIGURES



FIGURE 1.1 ANNUAL ENERGY CONSUMPTION DATA. ³	2
FIGURE 1.2 ANNUAL OIL PRODUCTION DATA. ⁴	2
FIGURE 1.3 ANNUAL CRUDE OIL PRICES REPRESENTED BY CURRENT CURRENCY AND MONEY OF THE DAY CURRENCY. ⁴	3
FIGURE 1.4 PRODUCTION OF HMF, FROM CELLULOSE AND CARBOHYDRATES, SERVES AS FEEDSTOCK FOR A RANGE OF CHEMICALS AND LIQUID FUELS. ⁸	6
FIGURE 2.1 ZIF BOND ANGLES CORRESPONDING TO ZEOLITE BOND ANGLES. ³⁰ ..	10
FIGURE 2.2 PHENOMENA OF TRANSPORT INVOLVED IN (A) WET IMPREGNATION AND (B) DRY IMPREGNATION. THE SOLUTE MIGRATES INTO THE PORE FROM THE LEFT TO THE RIGHT OF THE FIGURES. ³⁷	12
FIGURE 2.3 PHENOMENA OF TRANSPORT INVOLVED IN (A) THE CONSTANT-RATE PERIOD OF DRYING AND (B) THE FALLING-RATE PERIOD OF DRYING. THE SOLVENT MIGRATES FROM THE LEFT TO THE RIGHT OF THE FIGURES. ³⁷	13
FIGURE 2.4 SYNTHETIC ROUTES TO OBTAIN DMF FROM HMF. ⁴⁸	15
FIGURE 4.1 REACTION SYSTEMS USED IN THE EXPERIMENT. (METHOD 1) BATCH REACTIONS, (METHOD 2) SEMI-BATCH REACTIONS.	24
FIGURE 4.2 PROCEDURE FOR THE SYNTHESIS OF ZIF-67.	29
FIGURE 4.3 PROCEDURE FOR THE CONVERSION OF ZIF-67 TO Pd/CoNC.....	29
FIGURE 4.4 INCIPIENT WETNESS IMPREGNATION METHOD FOR THE DEPOSITION OF PALLADIUM ON CoNC.....	30
FIGURE 4.5 SEM IMAGES OF ZIF-67 SIZE CONTROL OF ZIF-67 WITH DIFFERENT ORGANIC LINKER TO METAL SOURCE RATIO.....	32
FIGURE 4.6 SEM IMAGES OF ZIF-67 UNDER 500 NM MAGNIFICATION.....	32
FIGURE 4.7 SEM IMAGES OF CoNC UNDER DIFFERENT CARBONIZATION TEMPERATURES.....	34
FIGURE 4.8 SEM-EDS MAPPING IMAGES SHOWING HOMOGENEOUS DISTRIBUTION OF Co AND Pd ON THE MATERIAL.	36
FIGURE 4.9 ZIF-67 TEM IMAGES THROUGH DIFFERENT MAGNIFICATIONS.....	38
FIGURE 4.10 TEM IMAGE OF CoNC.	39
FIGURE 4.11 TEM SELECTED-AREA ELECTRON DIFFRACTION PATTERNS OF CoNC.	

.....	39
FIGURE 4.12 TEM IMAGE OF Pd/CoNC.....	40
FIGURE 4.13 Pd/CoNC WITH COBALT AND PALLADIUM PARTICLES SHOWN.....	40
FIGURE 4.14 FOCUSED TEM IMAGE ON COBALT PARTICLE.	41
FIGURE 4.15 FOCUSED TEM IMAGE ON PALLADIUM PARTICLE.	41
FIGURE 4.16 N ₂ ADSORPTION/DESORPTION ISOTHERM OF ZIF-67.	42
FIGURE 4.17 N ₂ ADSORPTION/DESORPTION ISOTHERM OF CoNC.	43
FIGURE 4.18 XRD PATTERN OF ZIF-67 UNDER DIFFERENT PRECURSOR RATIOS. .	44
FIGURE 4.19 XRD PATTERN OF ZIF-67 AND CoNC.	45
FIGURE 4.20 STANDARD XRD PATTERN OF COBALT.	45
FIGURE 4.21 MAGNETISM DEMONSTRATED IN CoNC.....	46
FIGURE 4.22 WEIGHT LOSS PROFILE OF ZIF-67 TO CoNC CONVERSION.	47
FIGURE 4.23 CALIBRATION CURVE FOR DMF.	48
FIGURE 4.24 CALIBRATION CURVE FOR MFAD.	48
FIGURE 5.1 YIELD OF DMF VARYING CATALYST AMOUNTS. 4.5 mL THF IN 7 mL VIAL, 0.05 G HMF, 0.06 G NABH ₄ , 1 mL DI WATER, 303K.....	50
FIGURE 5.2 YIELD OF DMF VARYING REACTION TEMPERATURES. 4.5 mL THF IN 10 mL VIAL, 0.05 G HMF, 0.06 G NABH ₄ , 1 mL DI WATER, 0.1 G CATALYST.	50
FIGURE 5.3 DMF YIELD VARYING REACTION TIME. 4.5 mL THF IN 10 mL VIAL, 0.05 G HMF, 0.06 G NABH ₄ , 1 mL DI WATER, 0.1 G CATALYST.	52
FIGURE 5.4 DMF YIELD VARYING REACTION TIME. 4.5 mL THF IN 7 mL VIAL, 0.05 G HMF, 0.06 G NABH ₄ , 1 mL DI WATER, 0.1 G CATALYST.	52
FIGURE 5.5 DMF YIELD WITH OR WITHOUT NaOH ADDITION. 4.5 mL THF IN 7 ML VIAL, 0.05 G HMF, 0.06 G NABH ₄ , 0.14 ML DI WATER + NaOH, 0.1 G CATALYST, 3 HR.	54
FIGURE 5.6 DMF YIELD WITH NaOH ADDITION VARYING TEMPERATURE. 4.5 ML THF IN 7 ML VIAL, 0.05 G HMF, 0.06 G NABH ₄ , 0.14 ML DI WATER + NaOH, 0.1 G CATALYST, 3 HR.	54
FIGURE 5.7 DMF YIELD WITH Pd AND Co LOCATION VARIATION. 4.5 mL THF IN 7 ML VIAL, 0.05 G HMF, 0.06 G NABH ₄ , 1 mL DI WATER, 303K.....	58
FIGURE 5.8 SCHEME FOR BATCH AND SEMI-BATCH REACTIONS DETERMINING THE TIMING FOR THE ADDITION OF SODIUM BOROHYDRIDE.....	60
FIGURE 5.9 COMPARISON OF BATCH OR SEMI-BATCH YIELDS.	60

FIGURE 5.10 DMF YIELD WITH OR WITHOUT H ₂ SO ₄ ADDITION. 4.5 mL THF IN 20 mL VIAL, 39 mL MFAD, 0.06 G NABH ₄ , 30 WT% NAOH SOLUTION IN PUMP, 0.1 G CATALYST, 303K, 0.34 mL/HR FOR 3 HR, THEN 1 HR REACTION TIME. (8 mL H ₂ SO ₄ ADDED IF REQUIRED.)	61
FIGURE 5.11 DMF YIELD WITH ADDITION OF VARYING AMOUNTS OF H ₂ SO ₄ . 4.5 mL THF IN 10 mL VIAL, 39 mL MFAD, 0.06 G NABH ₄ , 30 WT% NAOH SOLUTION IN PUMP, 0.1 G CATALYST, 303K, 0.34 mL/HR FOR 3 HR, THEN 1 HR REACTION TIME.....	62
FIGURE 5.12 DMF YIELD STARTING WITH DIFFERENT REACTANTS. 4.5 mL THF IN 10 mL VIAL, 0.06 G NABH ₄ , 30 WT% NAOH SOLUTION IN PUMP, 0.1 G CATALYST, 303K, 1 ATM, 0.34 mL/HR FOR 3 HR, THEN 1 HR REACTION TIME. (EQUAL MOL OF REACTANT).....	63
FIGURE 5.13 ATMOSPHERIC AND NON-ATMOSPHERIC PRESSURE TESTS.	64
FIGURE 5.14 COMPARISON OF CATALYST WITH PALLADIUM OR COBALT ONLY.	65

LIST of TABLES



TABLE 2.1 PAST WORKS ON DMF SYNTHESIS.....	19
TABLE 4.1 PARTICLE SIZE OF ZIF-67 UNDER DIFFERENT PRECURSOR RATIOS.	33
TABLE 4.2 SEM-EDS ANALYSIS OF ZIF-67.....	35
TABLE 4.3 SEM-EDS ANALYSIS OF CoNC.....	35
TABLE 4.4 SEM-EDS ANALYSIS OF Pd/CoNC.....	36
TABLE 4.5 CoNC UNDER DIFFERENT CALCINATIONS TEMPERATURES.	43
TABLE 5.1 YIELD OF DMF STARTING FROM DIFFERENT REACTANTS.	56

1. INTRODUCTION



1.1. Energy Crisis

The diminishing supply of fossil fuel calls for the rise of alternative energy sources. As Jevons Paradox proposed in 1865, the demand for energy would only increase even if energy-saving or efficient devices were invented. Reasons could be attributed to the ever increasing population or the advancement of technology and the high demand for luxurious lifestyles.

On Figure 1.1, China was taken as an example, since it is currently one of the most intensely developing countries. The energy consumption has increased by 106 Million Tonnes of Oil Equivalent from 2012 to 2013. The International Energy Agency and the Organization for Economic Co-operation and Development has defined one Toe to be equal to 41.868 GJ.^{1,2} As the demand for energy continues to increase, there has to be other sources of energy, because it is now common knowledge that petroleum reserves would one day run out.

China

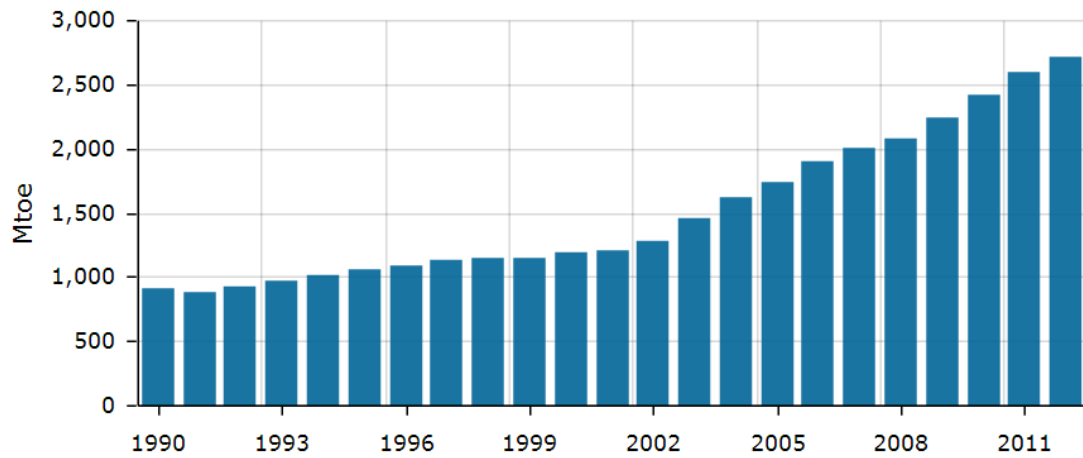


Figure 1.1 Annual energy consumption data.³

Production by region

Million barrels daily

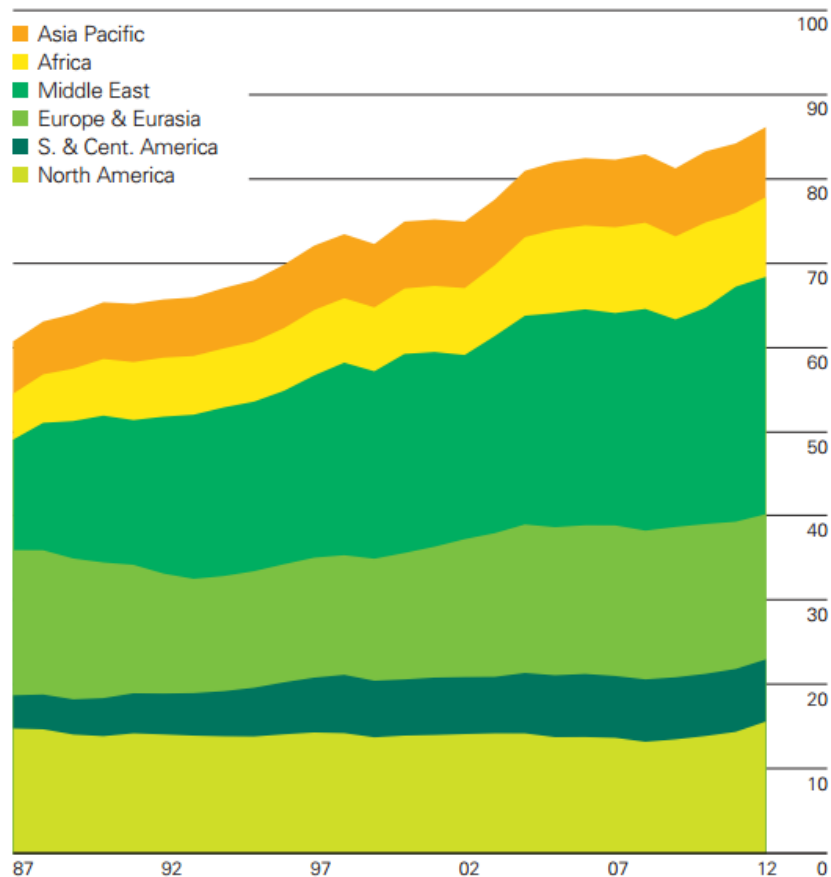


Figure 1.2 Annual oil production data.⁴

Even though Figure 1.2 shows that the production of oil is still rising as of now,

it can be seen in Figure 1.3 that the price of oil is also increasing significantly. It is therefore ideal to find other sources of energy that could replace or relieve the intense use of fossil fuels.

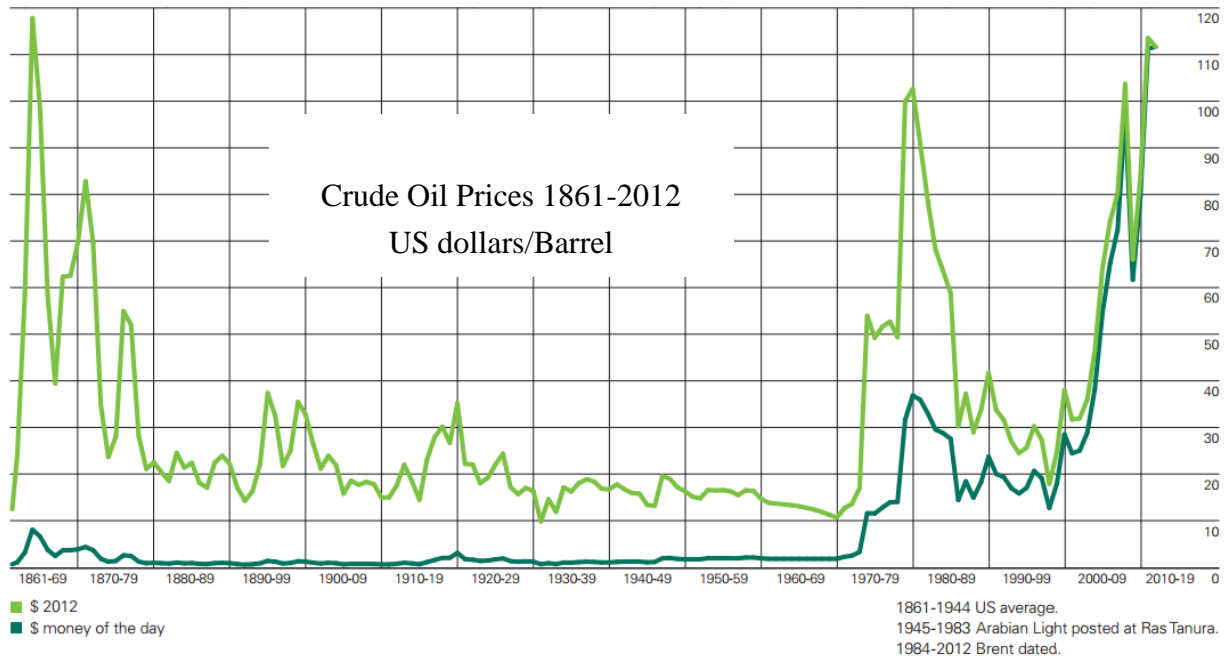
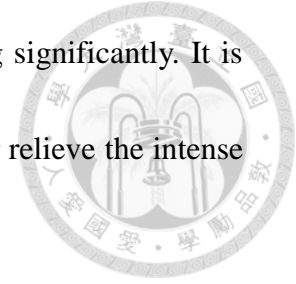
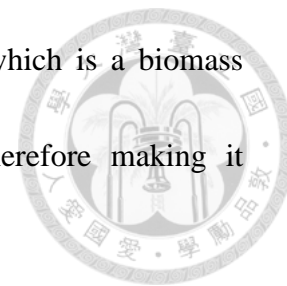


Figure 1.3 Annual crude oil prices represented by current currency and money of the day currency.⁴

Extensive research has been done on alternatives to fossil fuels. Solar, wind, hydro and geothermal energy comes to mind, however, these alternatives are dependent on the geology, time of day, or maybe even seasonal changes. A more transferable or stable source of energy has to be realized. Biomass holds many of these fine qualities to make it a suitable candidate. Biomass absorbs and stores solar

energy chemically, making it stable. 2,5-Dimethylfuran (DMF), which is a biomass derived fuel, holds properties that are similar to gasoline, therefore making it incentive to study the production of DMF.^{5,6}

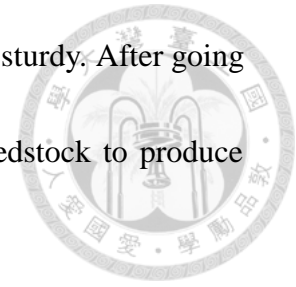


1.2. Biomass development

The development of biomass can be categorized into three generations. The first generation of biomass utilizes agricultural crops because their composition contains high lipid/oil or sugar contents. Biodiesel and bioethanol can be produced from these crops. Over the last few decades, innumerable works have been published regarding the conversion of this feedstock to energy. However, the competition of using this feedstock for energy and using them as our food supply makes it difficult to rely on this source.

Second generation biomass utilizes agricultural wastes that are also high in lipid/oil and sugar content. These agricultural wastes are often lignocellulosic matter. Lignocellulose is composed of Cellulose, Hemicellulose and Lignin. Lignocellulosic biomass is a viable option in that (a) it is abundantly available on earth, (b) it does not coincide with our food supply, (c) a positive net energy gain (NEG) can be obtained from the conversion process. Similar products such as biodiesel and bioethanol could also be produced from lignocellulose. The key difference lies in that lignocellulose is

composed of strongly polymerized structures that are recalcitrantly sturdy. After going through hydrolysis, the collected sugar units could be used as feedstock to produce fuel.



Third generation biomass utilizes micro-algae as the main source of feedstock. This feedstock is also largely dependent on the geology and environment, since large masses of micro-algae has to be able to be grown for this alternative to be realized. Since this research does not focus on third generation biomass, it will be concluded here that second and third generation biomass does not conflict with each other and there is no clear winner of these two, it all depends on the geology and environment of the production site.

1.3. Biomass Conversion

As Figure 1.4 has shown, Cellulose (A component of Lignocellulose) can be hydrolyzed into glucose, and then Glucose can be isomerized into Fructose. Lastly, fructose can be dehydrated into 5-Hydroxymethylfurfural (HMF), a reactant in which a lot of the building block chemical synthesis works have been based on. Numerous works have been done on the hydrolysis of Cellulose into glucose. Even direct hydrolysis of raw crops has been researched quite extensively over the past few years.⁷

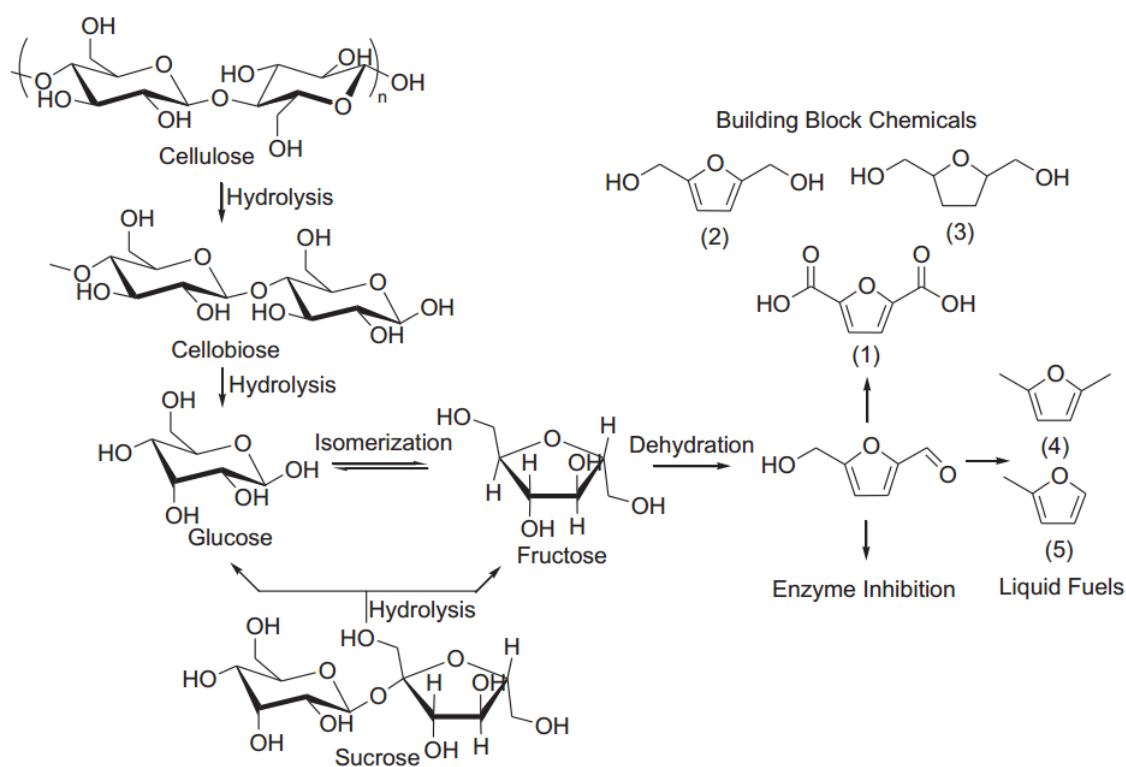
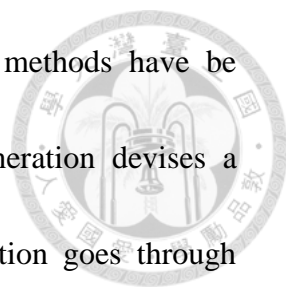


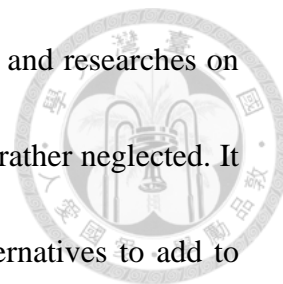
Figure 1.4 Production of HMF, from cellulose and carbohydrates, serves as feedstock for a range of chemicals and liquid fuels.⁸



Three generations of biomass pretreatment and hydrolysis methods have been categorized in a review by Sathitsuksanoh et al.⁹ The first generation devises a one-step biomass dissolution and hydrolysis. The second generation goes through biomass dissolution first, followed by enzymatic hydrolysis. The third generation utilizes lignocellulose fractionation. The first generation is mainly based on the use of concentrated acids, which is raw-material independent, however it poses some disadvantages, such as product separation difficulties, acid recovery and acid re-concentration.¹⁰⁻¹² The second generation mainly focuses on the use of enzymes; the use of enzymes could overcome some of the difficulties faced by the first generation, however, other problems such as high costs, corrosive and toxic properties of pretreatment solvents.^{13,14} Third generation methods involve the use of fractionation, overcoming separation difficulties faced by the first generation methods, fractionation could achieve continuous processes through the use of acids and ionic liquids under modest reaction conditions.^{15,16}

Works on the isomerization of glucose to fructose or even cellulose oligomers to fructose have been done.¹⁷ Particularly, work on cellulose-to-HMF conversion have been studied extensively over the past few years and high yields could also be achieved.¹⁸⁻²² Selection of the most suitable method could be made over large quantities of works for the production of HMF, one-step or one-pot synthesis methods

are also now available. However, despite large quantities of works and researches on the synthesis of HMF, the research on the synthesis of DMF seems rather neglected. It is therefore what this research aims to search for options and alternatives to add to works on DMF synthesis.



2. PAPER SURVEY



2.1. Metal Organic Framework (MOF) based catalysts

Metal Organic Frameworks are inorganic (Metal component) and organic units linked together to form a structure with high degrees of crystallinity. It has recently gained widespread popularity due to its versatility to be shaped differently through the use of different metal nodes and linkers, which often give them different properties or functionalities. Often compared with Zeolites, MOFs show similar characteristics to Zeolites. Generally, MOFs are thermal and chemically stable, and contain micropores which grant them large surface areas of 1000 to 10,000 m²/g. Recently, Postsynthetic Modification (PSM) through covalent bond exchanges of MOFs have also been studied to make MOFs even more versatile in terms of applications.²³ With these attractive characteristics, MOFs can be applied to a wide variety of applications such as gas storage, gas separation, catalysis and sensors.²⁴ Over the last decade, MOFs have been widely explored as potential catalysts.²⁵⁻²⁹ Specifically, the class of Zeolitic Imidazolate Frameworks (ZIF) will be discussed here, since the catalyst used here is derived of such origins.

As suggested by the name, ZIF uses imidazolate units as linkers to form a structure with M-Im-M angles of 145°, similar to Si-O-Si angles in Zeolites. ZIF

possesses tetrahedral topologies

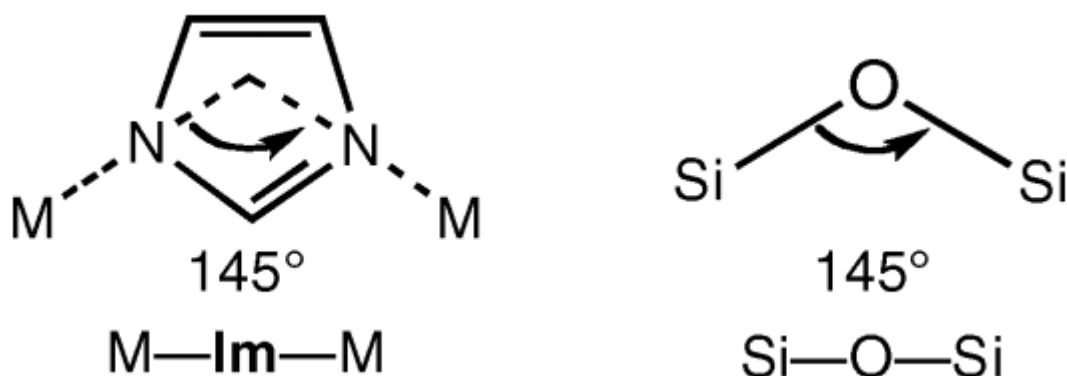


Figure 2.1 ZIF bond angles corresponding to Zeolite bond angles.³⁰

The specific material used in this research is ZIF-67, it was chosen because it contains Cobalt as the metal node, which would be used to catalyze the catalysis of hydrogen production from sodium borohydride.³¹ The synthesis of ZIF-67 and its calcination into cobalt supported on carbon has also gained attention quite recently.³²⁻³⁶ It is convenient to have the cobalt metal homogeneously distributed on the product, rather than using different methods to load the metals onto the material.

2.2. Incipient Wetness Impregnation³⁷



One of the most widely used industrial methods of preparing supported precious metal catalysts combines impregnation and drying. This is a relatively easy method that deposits metals onto supports through physical means. Impregnation is when the liquid phase comes into contact with a solid phase, and the liquid phase is absorbed by the solid phase. A typical impregnation involves allowing a precursor solution containing the metal source to be absorbed into a solid support. The precursor is chosen according to the price and its physicochemical properties. The affinity of the precursor towards the solid support will determine the effect of the impregnation. The particle size of the precursor is also a determining factor, since its interaction with the pore of the solid will determine the effect of the impregnation.

$$J = -D \frac{\partial \phi}{\partial x} \quad \text{Fick's Law}$$

$$Q = \frac{-kA (P_b - P_a)}{\mu L} \quad \text{Darcy's Law}$$

When the liquid phase volume exceeds the volume of the pores on the support, wet/diffusional impregnation is given as the name of the method.³⁸⁻⁴² Fick's law of diffusion, the adsorption capacity of the surface and the adsorption equilibrium constant governs this type of impregnation. When the liquid phase volume is equal to the volume of the pores on the support, the method is named dry impregnation. For

this type of impregnation, other effects come into play, such as the pressure driven capillary flow of the solute inside the pores. Figure 2.1 shows these phenomena in illustration. This phenomenon can be described by Darcy's Law.

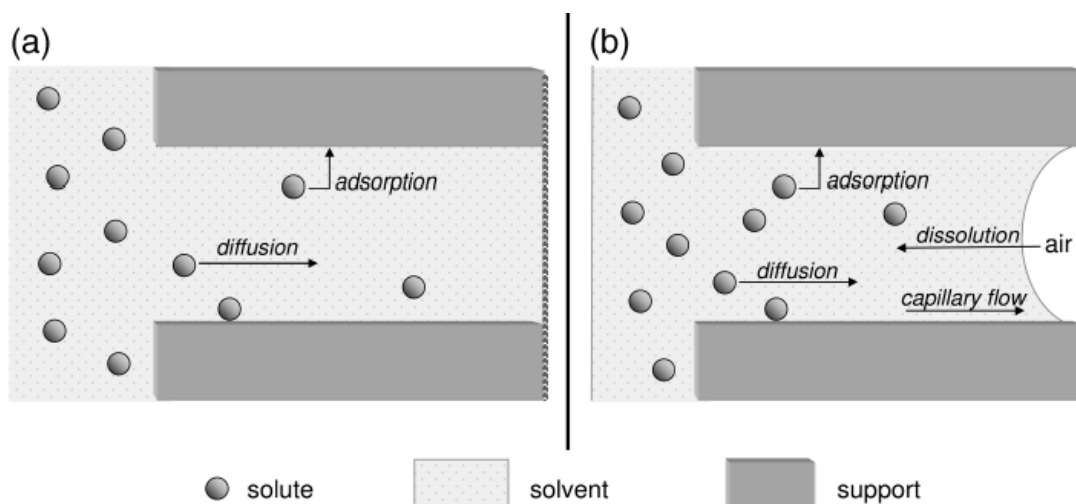
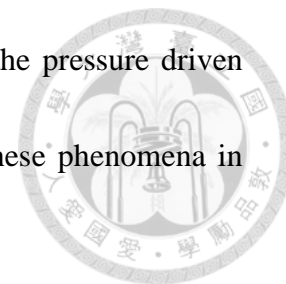


Figure 2.2 Phenomena of transport involved in (a) wet impregnation and (b) dry impregnation. The solute migrates into the pore from the left to the right of the figures.³⁷

When the precursor solution is impregnated inside the pores of the support, the mixture is dried to remove the solvent, while the metal stays inside the pores of the support. Typical procedures involve heating in an oven to the boiling point of the solvent with or without selected gas flows. Heating rate and final heating temperatures can all affect the adsorption of the precursor on the pore surfaces. The balance between adsorption, back-diffusion and convection determines the

distribution of the precursor inside the pores.⁴³⁻⁴⁶ When the convective flow of the solvent counters the vapor removal flow, a constant-rate period is achieved as shown in Figure 2.2(a). This is usually the case when the heating rate and the drying temperature are high, the solvent front recedes into the pores and the evaporation occurs inside the pores. When the convective flow is slower than the vapor removal flow, a falling-rate period is achieved as shown in Figure 2.2(b). This is usually the case when the heating rate and the drying temperature are low, the solvent front stays at the surface of the support and loss of the precursor particles can occur through microconvection. The drying regime is defined as slow if the constant-rate period predominates, and as fast if it is the falling-rate period.

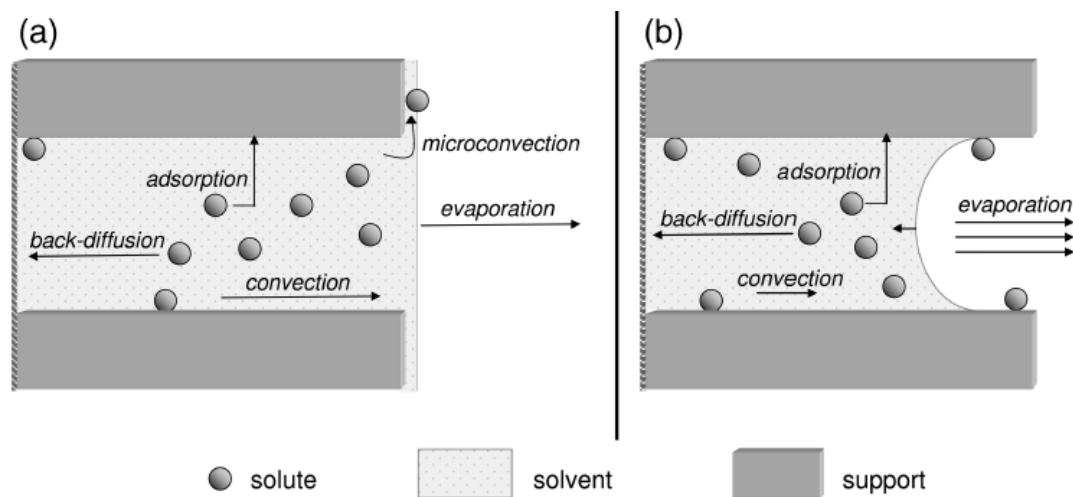
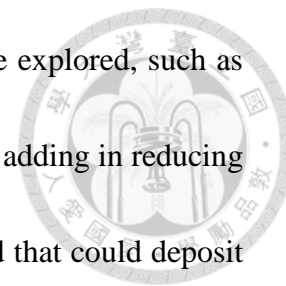


Figure 2.3 Phenomena of transport involved in (a) the constant-rate period of drying and (b) the falling-rate period of drying. The solvent migrates from the left to the right of the figures.³⁷

Other methods of metal deposition onto the supports could be explored, such as the stirring of the support in metal precursor solutions all the while adding in reducing agents to deposit the metal onto the supports. A convenient method that could deposit metal with an even distribution onto the supports would be attractive. Deposition to form chemical bonds between support and metals would also help make the metals more firmly attached on the material, which could lead to good recyclability.



2.3. Production of 2,5-Dimethylfuran

It has been proposed that the production of DMF from HMF will go through two pathways as shown in Figure 2.4. Both of these pathways involve the hydrogenation and hydrogenolysis of HMF and its intermediates.⁴⁷

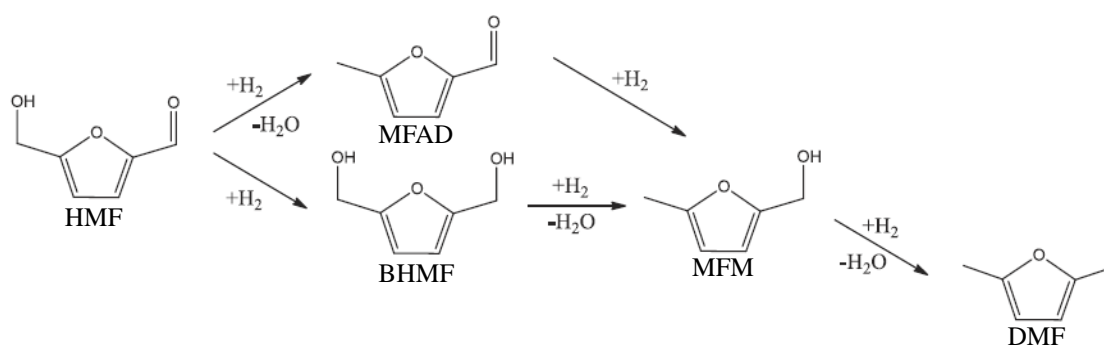


Figure 2.4 Synthetic routes to obtain DMF from HMF.⁴⁸

Since HMF is a widely known chemical platform, most of the works on DMF synthesis has been conducted starting with HMF. HMF is a chemical platform that is often synthesized from hexoses such as fructose through dehydration reactions. Earlier works of DMF synthesis often start with fructose. Herein, focus will be put on HMF to DMF conversions.

Sudipta and Basudeb et al. synthesized DMF from HMF in a sequential reaction that starts with fructose.⁴⁹ A yield of 32% DMF could be achieved from fructose under conditions stated in Table 2.1. Binder and Raines et al. also synthesized DMF from HMF in a sequential reaction that starts from fructose.⁵⁰ The reaction conditions

were a follow up of the work of Román-Leshkov and Dumesic et al.⁴⁷ A yield of 32.5% DMF could be achieved from fructose in this work. Chidambaram and Bell et al. demonstrated tests in ionic liquid systems and obtained a yield of 32% DMF under EMIMCl with addition of acetonitrile.⁵¹ It is mentioned in their work that the solubility of hydrogen inside the solvent is a determining factor for the efficiency of the hydrogenation reaction. Under the same conditions they compared four different metals for DMF synthesis which are Palladium, Platinum, Ruthenium and Rhodium. They found that Carbon supported Palladium shows the best results.

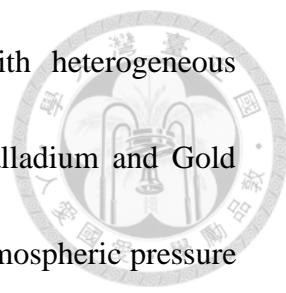
Thananathanachon and Rauchfuss et al. used Pd/C as catalyst with formic acid as a liquid hydrogen source and deoxygenation agent at the same time.⁵² A different term was given for aqueous hydrogenations, which is transfer hydrogenation, distinction of this mechanism with traditional hydrogenation can be made by determining whether hydrogen gas is produced or not. Transfer hydrogenation does not need production of hydrogen gas; traditional hydrogenations require production of hydrogen gas. The novelty of this work resides in that no pressured hydrogen gas is needed, which saves a lot of energy. Jungho and Dionisios et al. used Ru/C catalyst with 2-propanol as hydrogen source for transfer hydrogenation.⁵³ It is claimed in their work that no homogeneous acid is used in the reaction as compared to the work of Thananathanachon's group. They mentioned that using 2-propanol as a hydrogen

donor is attractive due to its green derivation. Alcohols can be readily produced from biomass and the dehydrogenated products can be recycled by hydrogenation, although this requires yet another step with hydrogenation.



Regarding works on using Ru/C as a catalyst, Junhua and Shijie et al. demonstrated that 60.3% DMF yield could be obtained under the conditions in Table 2.1.⁵⁴ Yanhong and Yanqin et al. used Ru/Co₃O₄ as catalyst to obtain high yields of 93.4% DMF under the conditions in Table 2.1.⁴⁸ It is reported in their work that Ruthenium plays the role of carbonyl group to hydroxyl group conversion. In fact, most of the works have reported that carbonyl to hydroxyl group conversions can be done easily, where they proposed that C-O bond cleavage (hydrogenolysis) is the determining step. Therefore they used Co₃O₄ as the catalyst for C-O bond cleavage.

One of the earliest works on DMF synthesis dates back to 2007, where Román-Leshkov and Dumesic et al. synthesized DMF starting from either fructose or HMF.⁴⁷ A bimetallic copper and ruthenium catalyst (Cu-Ru/C) was used for the conversion of HMF to DMF. They proposed that due to the copper having lower surface energy than ruthenium, a two-phase system develops on the catalyst in which the copper coats the ruthenium. This was needed because during their sequential reaction from fructose to HMF, chloride ions were present, and poisoning of the copper on the catalyst could occur.⁵⁵ Yields of 71% DMF could be achieved in



purified solvents with chloride ions absent. Another work with heterogeneous bimetallic catalyst by Nishimura and Ebitani et al. introduces Palladium and Gold supported on Carbon.⁵⁶ They claim to achieve 96% yields under atmospheric pressure with moderate temperature as shown in Table 2.1. The presence of gold on the catalysts does indeed improve the yield as the reactants were increased and the catalyst amount was decreased. Huang and Fu et al used a bimetallic Nickel and Tungsten Carbide catalyst to catalyze the reaction under the reaction conditions given in Table 2.1.⁵⁷ It was reported in their work that Nickel shows excellent hydrogenation abilities, however its selectivity was bad therefore tests were conducted with tungsten carbide. Tungsten carbide shows excellent selectivity towards the hydrogenolysis of alcohol groups into methyl groups, basically a deoxygenation reaction. This leads them to come up with a catalyst that contains lower amounts of Nickel for the conversion of HMF to an intermediate with both hands switched into alcohol groups then the high amount of Tungsten Carbide would convert the alcohol groups into methyl groups producing DMF. In the last work on bimetallic catalysts to date, Wang and Schuth et al made a catalyst of Platinum and Cobalt nanoparticles encased in hollow carbon nanospheres and conducted the reaction under the conditions listed in Table 2.1.⁵⁸ They have attributed the high yield of 98% to the interaction between the Cobalt and Platinum alloy, because tests with Platinum or Cobalt supported alone

resulted in low yields.



Table 2.1 Past Works on DMF Synthesis.

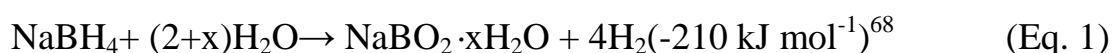
Catalyst	Reactants	Reaction Condition	DMF Yield [%]	Ref
Cu-Ru/C (79 mg)	HMF	H ₂ (6.8 bar), 220°C, 10h	49	50
Pd/C (2.13 mg Pd)	HMF (126 mg), EMIMCl, acetonitrile	120°C, H ₂ (62 bar), 1h	15	51
Pd/C (0.4 g)	HMF (0.25 g), FA (0.78 mL), H ₂ SO ₄ (14 mL), THF (10 mL)	70°C, 15 h	95	52
Ru/C (0.8 g)	THF (10 mL), H ₂ SO ₄ (35 μL)	75°C, 15h	24	49
Cu-PMO (100 mg)	HMF (100 mg), ScMeOH (3 mL)	260°C, 3h	48	59
Ru/Co ₃ O ₄ (0.1 g)	HMF (0.25 g), THF (10 mL)	H ₂ (0.7 MPa), 130°C, 24h	93.4	48
Cu-Ru/C (0.75 g)	HMF (2.5 g), Cu:Ru = 3:1, 1-butanol (47.5 g)	260°C, H ₂ (6.8 bar), 10h	71	47
Pd/C	HMF: Pd/C = 5:1, H ₂ O:CO ₂ = 0.32:1, H ₂ O (1 mL)	H ₂ (1 MPa), ScCO ₂ (10 MPa), 80°C, 2h	100	60
Ru/C (20 wt%)	HMF (0.75 g), <i>n</i> -butanol (25 mL)	H ₂ (0.01475 mol/g HMF), 260°C, 1.5h	60.3	54
Ru/C (100 mg, 5 wt%)	HMF (240 mg), 2-propanol (24 mL)	N ₂ (2.04 MPa)	81	53
7Ni-30W2C/AC (120 mg)	HMF (1 mmol), THF (12 mL)	H ₂ (4MPa), 180°C, 3h	96	57
Pd ₅₀ Au ₅₀ /C (31.3 mg)	HMF (1 mmol), THF (10 mL)	H ₂ (1atm, 4L), 60°C, 12h	96	56
Pt-Co@HCS (50 mg)	HMF (2mmol), Butanol	H ₂ (10bar), 180°C, 2h	98	58

3. OBJECTIVE



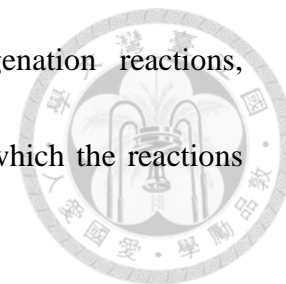
The core idea of this research stems from the functions of our catalyst. Our catalyst contains Palladium and Cobalt, as the name Pd/CoNC implies. It is textbook and common knowledge that precious metals such as Pt, Pd and Ru provide a surface for which hydrogenation reactions occur.⁶¹⁻⁶⁴ It is therefore suitable that we apply our catalyst to hydrogenation reactions. Hydrogenation reactions require a source of hydrogen whether it comes from directly supplying the system with hydrogen gas or indirect methods such as transfer hydrogenation.⁶⁵⁻⁶⁷

Sodium Borohydride (NaBH₄) is known to be able to produce hydrogen gas when reacted with water as shown in Eq. 1.^{20,21} This means that the production of hydrogen occurs inside the solution, which possibly provides a higher chance of contact between hydrogen atoms and the reaction sites, therefore NaBH₄ has been chosen as our source of hydrogen.



It is known that Cobalt can catalyze the hydrolysis of NaBH₄ solution to have a higher hydrogen generation rate and produce a larger total amount of hydrogen.⁶⁹⁻⁷³

Therefore our catalyst shows bifunctionality towards hydrogenation reactions, producing hydrogen at a faster rate and providing a surface for which the reactions can occur.



The chosen reaction for our research is the conversion of 5-methylfurfural to 2,5-Dimethylfuran. As discussed in the paper survey section. This reaction requires two hydrogenation reactions in total, of which one is the conversion of an aldehyde group to an alcohol group and the other is a hydrogenolysis reaction.

The objective of this research is to achieve a facile method of 2,5-Dimethylfuran synthesis under atmospheric pressure and room temperature while using an aqueous hydrogen source to obtain high yields. The advantages of atmospheric pressure and room temperature are that it provides a safe environment for synthesis, since highly pressured hydrogen gas at high temperatures can be quite dangerous. The reaction is also energy efficient because it does not require additional heating and purging with pressurized hydrogen gas. The use of aqueous hydrogen sources other than transfer hydrogenation on biomass conversion will also be explored here for the first time.

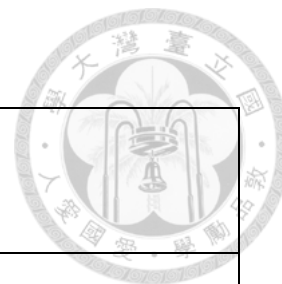
4. EXPERIMENTAL



4.1. Chemicals and Materials

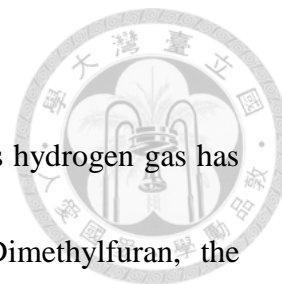
Chemical	Company
2,5-Bis(hydroxymethyl)furan (BHMF)	Polysciences
2,5-Diformylfuran(DF)	Aldrich
2,5-Dimethylfuran (DMF)	Aldrich
2-Methylimidazole	Aldrich
5-Hydroxymethylfurfural (HMF)	Aldrich
5-Methylfurfural (MFAD)	Aldrich
Carbon Supported Palladium (5 wt%)	Aldrich
Cobalt (II) Chloride Hexahydrate	Sigma-Aldrich
Hydrochloric Acid (HCl)	Sigma-Aldrich
Magnesium Sulfate (MgSO₄)	Yakuri Chemicals
Palladium (II) Chloride	Aldrich
Sodium Borohydride (NaBH₄)	Aldrich
Sodium Hydroxide (NaOH)	Sigma-Aldrich
Sulfuric Acid (H₂SO₄)	Sigma-Aldrich
Tetrahydrofuran (THF)	Sigma-Aldrich

4.2. Equipment



Equipment	Type
Centrifugator	Sigma 3-30KS
Ultrasonicator	Qsonica, Ultrasonic processor Part No.Q700
Lyophilizer	Eyela FDU-1200
Gas Chromatography-Mass Spectrometer- Flame Ionization detector (GC-MS)	HP-5ms
X-Ray Diffractometer (XRD)	Rigaku, Ultima IV
Specific Area and Pore Size Distribution Instrument	Micromeritics ASAP 2010
Scanning Electron Microscope (SEM)	Nova TM NanoSEM 230
TGA	PERKIN ELMER PYRIS 1
Syringe Pump	KDS-100
Calcination Oven	Thermoscientific Lindberg Blue M

4.3. Procedure for production of 2,5-Dimethylfuran



Owing to the fact that aqueous hydrogen source that produces hydrogen gas has been used here for the first time in the production of 2,5-Dimethylfuran, the experimental procedure was modified several times over the course of discovering the best system for the production of 2,5-Dimethylfuran. Two of the main reaction systems were discussed here:

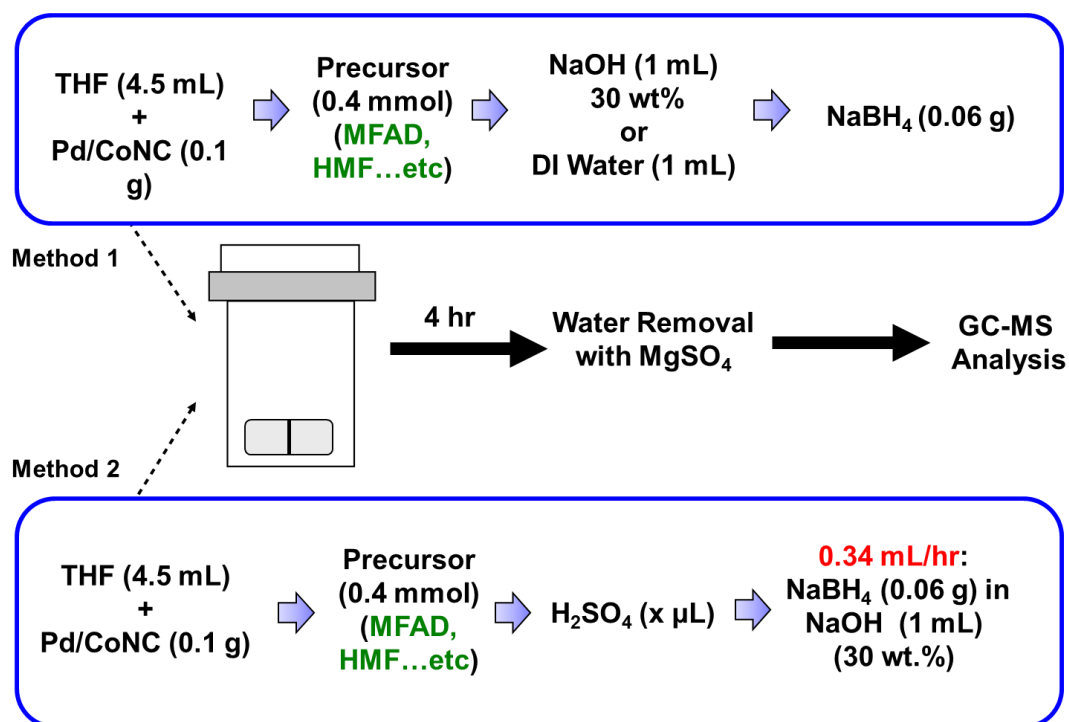
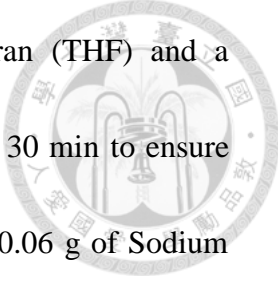


Figure 4.1 Reaction systems used in the experiment. (Method 1) Batch Reactions, (Method 2) Semi-Batch Reactions.

4.3.1. Batch Reactions

For a standard experiment procedure, 0.4 mmol of 5-methylfurfural (MFAD),



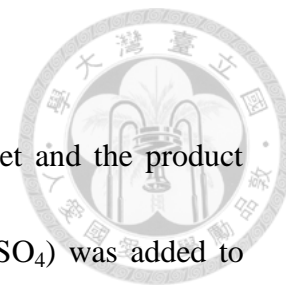
varying amounts of Pd/CoNC catalyst, 4.5 mL of tetrahydrofuran (THF) and a magnetic stir bar were added in a 7 or 10 mL vial to be stirred for 30 min to ensure quality distribution of the reactant throughout the catalyst surface. 0.06 g of Sodium Borohydride (NaBH_4) was then added right before addition of 1 mL of de-ionized water into the vial. After the addition of water, there would be intense bubbling, so the cap should be sealed as soon as possible. Parafilm was wrapped around the cap to ensure no loss of hydrogen gas produced. The reaction was placed in a water bath of varying temperatures for varying durations of reaction.

For reactions with addition of Sodium Hydroxide (NaOH), the reactant was 5-Hydroxymethylfurfural (HMF) instead of MFAD. 4.5 mL of THF with 0.1 g of Pd/CoNC catalyst were added as with the procedure of standard tests. After 30 minutes of stirring, de-ionized water was added with NaOH (0.14 mL). It can be observed that there is mild bubbling. The vial was then put in a water bath of varying temperatures for 3 hours.

For reactions with addition of acids, the reactant was also HMF instead of MFAD. 4.5 mL of THF with 0.1 g of Pd/CoNC catalyst were added as with the procedure of standard tests. For the addition of H_2SO_4 , 1.6 μL of H_2SO_4 was added with 1 mL of de-ionized water after 30 minutes of stirring. For addition of HCl, 2 μL of HCl was added instead. The reaction was then put in a water bath of 30°C for 3

hours.

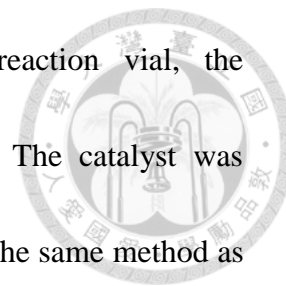
After the reaction, the catalysts were collected with a magnet and the product solution was poured into a 20 mL vial. Magnesium Sulfate (MgSO_4) was added to remove the water from the product solution for the safety of the Mass Spectroscopy. The MgSO_4 solid was filtered with a syringe and a filter disk. Finally, the solution was analyzed by GC-MS with the Agilent HP-5ms Column.



4.3.2. Semi-Batch Reactions

For semi-batch tests, 0.1 g of Pd/CoNC catalyst was prepared in a 10 mL vial with a magnetic stir bar. 0.4 mmol of MFAD was added with 4.5 mL of THF. The aqueous hydrogen source of NaBH_4 (0.06 g) in 30 wt% NaOH solution (1 mL) was prepared by addition of 0.14 mL of NaOH solution with 0.86 mL of de-ionized water in a 4 mL vial to create a basic environment. Then NaBH_4 was added to the solution, slow and minor bubbling can be observed. The solution was quickly transferred into a syringe on a syringe pump, while varying amounts of H_2SO_4 acid was added into the reaction vial. The reaction vial was then placed in a 30°C water bath and the NaBH_4 solution was introduced into the reaction vial (10 mL) with a syringe pump at an injection rate of 0.34 mL per hour. For atmospheric pressure tests, a syringe needle was placed on top of the reaction vial to achieve constant atmospheric pressure. After

the NaBH_4 solution (1 mL) was fully injected into the reaction vial, the hydrogenolysis reaction was performed for an additional hour. The catalyst was collected with a magnet and the product solution was treated with the same method as in batch reaction experiments. Finally, the solution was analyzed by GC-MS with the Agilent HP-5ms Column.



4.4. Catalyst Synthesis



The detailed synthesis methods are presented in the following paragraphs and several processes are shown in the figures below:

4.4.1. ZIF-67 Synthesis

To synthesize ZIF-67, 2-methyl imidazole (11.35 g) was dissolved in 40 mL deionized water and Cobalt(II) Chloride (0.4678 g) was dissolved in 4 mL deionized water. When 2-methyl imidazole was fully dissolved in water, aqueous Cobalt(II) Chloride was added into the 2-methyl imidazole solution. After stirring for five minutes at room temperature, the appearance of the mixture turns from carmine to purple. The solution was then centrifuged and washed with deionized water several times. The collected solid was then vacuum-dried in the lyophilizer overnight.

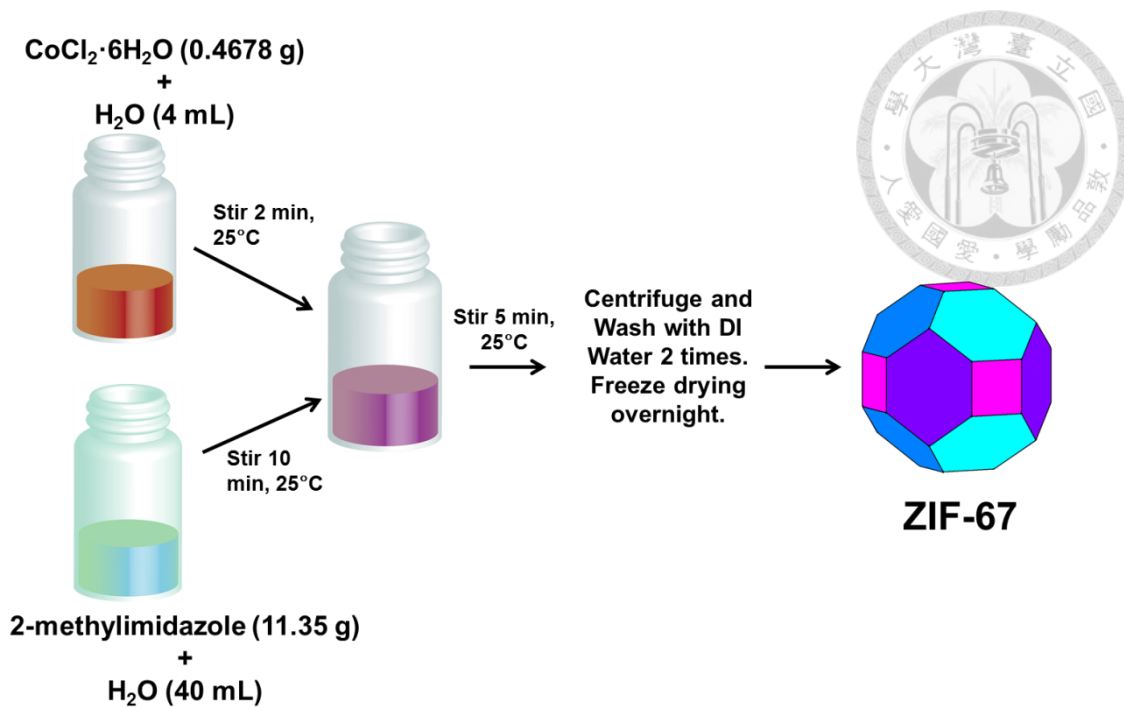


Figure 4.2 Procedure for the synthesis of ZIF-67.

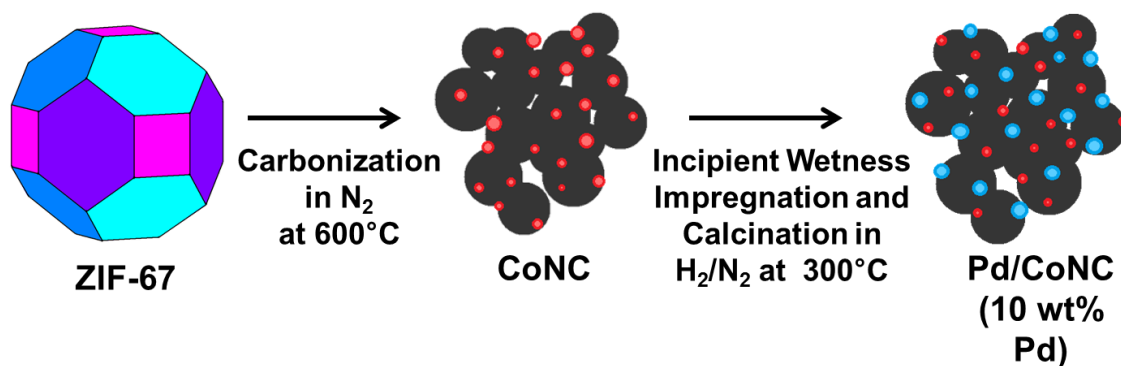


Figure 4.3 Procedure for the conversion of ZIF-67 to Pd/CoNC.

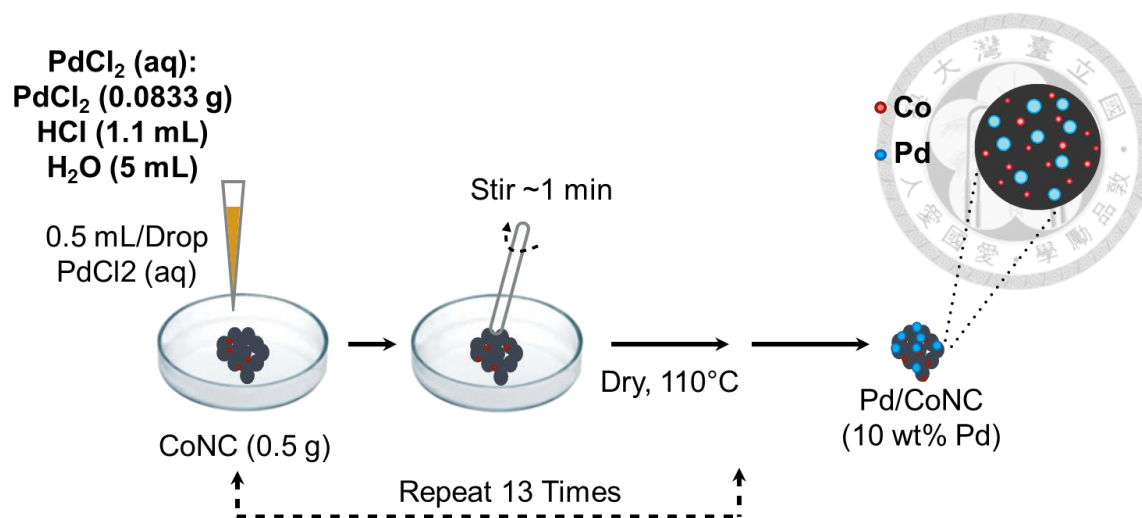
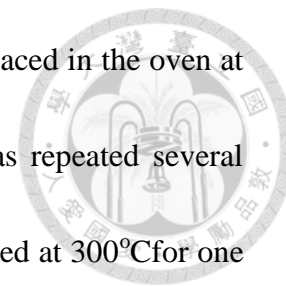


Figure 4.4 Incipient wetness impregnation method for the deposition of Palladium on CoNC.

4.4.2. ZIF-67 to Pd/CoNC Conversion

To remove 2-methyl imidazole from the solid and obtain cobalt on carbon, dried ZIF-67 was put in an oven and sintered under nitrogen flow. The sintering program starts from room temperature to 200°C with a heating rate of 5°C per minute. It was held at 200°C for 1 hour, and then heated to 600°C with a heating rate of 5°C per minute. After holding it at 600°C for 3 hours, it was cooled to room temperature and the collected solid was grinded to obtain Co/NC. The 10 wt% Pd/CoNC catalysts were prepared by incipient wetness impregnation, using an aqueous solution containing Palladium(II) Chloride. Palladium(II) Chloride (0.0833 g) was dissolved in 1.1 mL of concentrated HCl first, and then 5 mL of deionized water was added. The precursor solution with Pd^{2+} was dropped gradually (0.5 mL) onto the CoNC, keeping

an incipient wetness liquid/solid ratio of 1mL per gram and then placed in the oven at 110°C. To reach the desired content of Pd, the same method was repeated several times. After the impregnation process, the dried powder was calcined at 300°C for one hour with a heating rate of 5°C in H₂ (5 wt%) /N₂(95 wt%) flow to obtain Pd/CoNC as the final product.



4.5. Characterization

4.5.1. Scanning Electron Microscope (SEM)

The morphology of the samples was observed with SEM (NovaTM NanoSEM 230). All samples were dissolved in ethanol to form a clear solution followed by 5 min sonication. 10 uL of the sample-containing solution was dropped onto either a copper grid or carbon tape (200 mesh, Formvar-covered and carbon-coated). Before SEM observations, the grids were kept under vacuum and subjected to Pt coating for 120 seconds by sputtering at a current of 20 mA. SEM-EDS data was obtained using the same instrument.

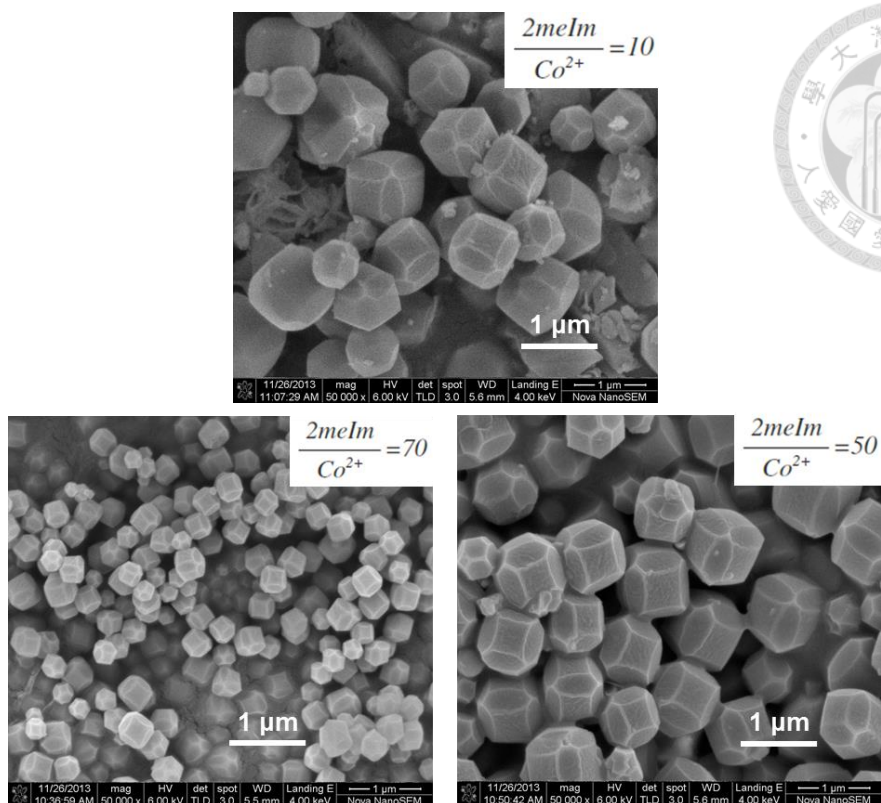


Figure 4.5 SEM images of ZIF-67 size control of ZIF-67 with different organic linker to metal source ratio.

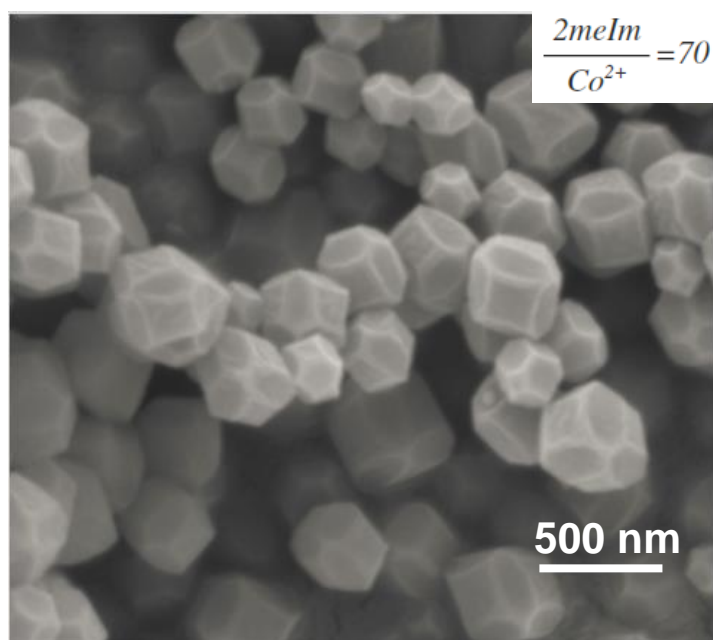


Figure 4.6 SEM images of ZIF-67 under 500 nm magnification.

As shown from Figure 4.4, we can see that size control of ZIF-67 particles is possible through the use of different organic linker to metal source ratios. We can also see from Table 4.1 organized below that a ratio of 70 equates to the smallest particle size, and a smaller particle size often equates to a larger surface area. Therefore we have selected a ratio of 70 as the optimum ratio.

Table 4.1 Particle size of ZIF-67 under different precursor ratios.

2-MeIm/Co²⁺	Diameter (nm)	Cubic Length (nm)
70	385	162
50	951	487
10	1080	488

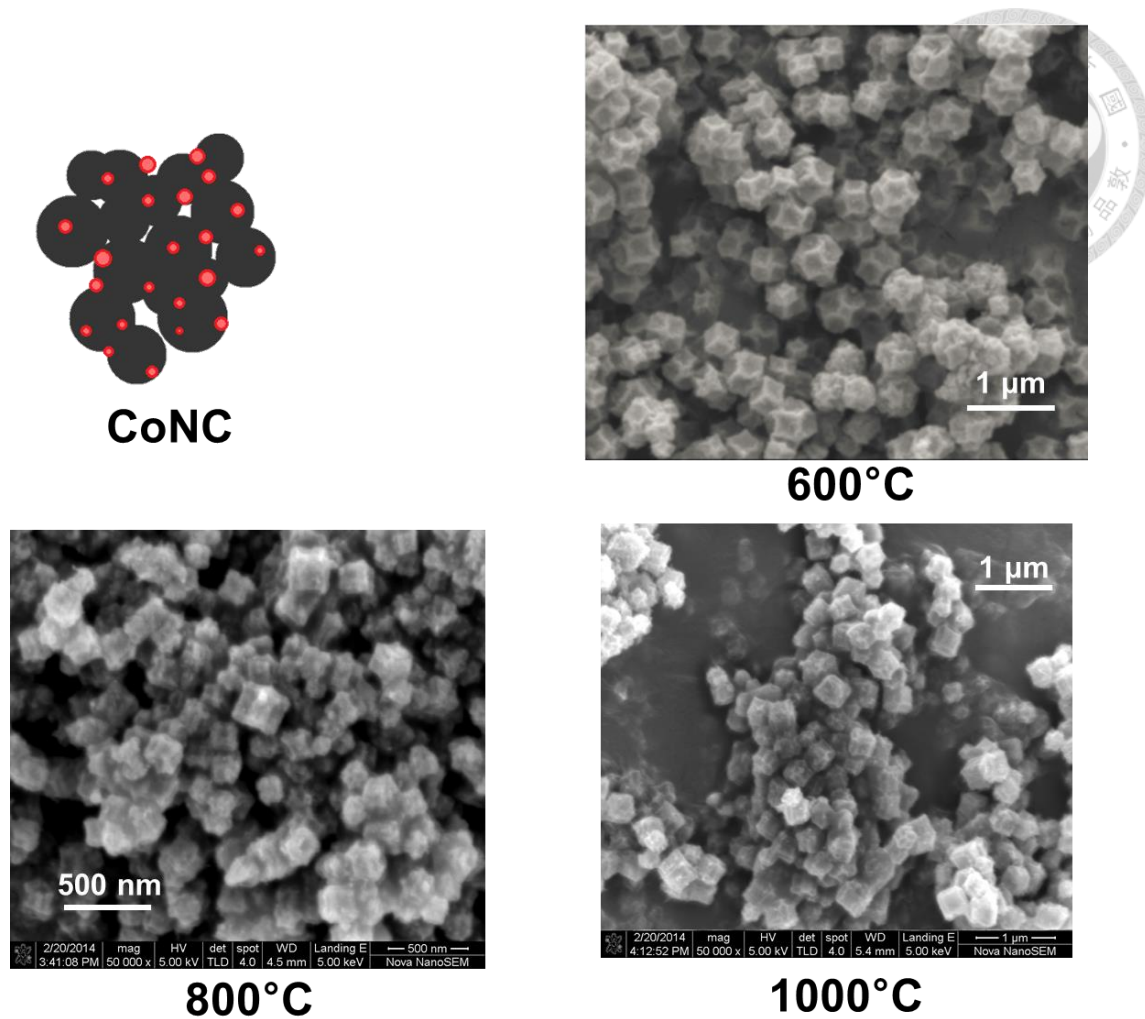
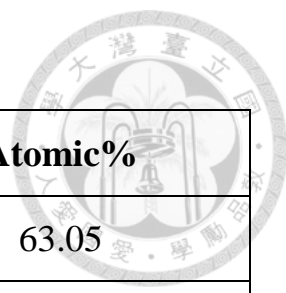


Figure 4.7 SEM images of CoNC under different carbonization temperatures.

As shown in the SEM images, it can be seen that calcination temperatures higher than 600°C destroys the uniform morphology of the CoNC particles. Therefore 600°C was chosen as the optimum temperature for the calcination of ZIF-67 into CoNC particles.

Table 4.2 SEM-EDS analysis of ZIF-67.



Element	Weight%	Atomic%
C K	49.89	63.05
N K	25.51	27.64
O K	4.31	4.09
Co L	20.29	5.23
Totals	100	

Table 4.3 SEM-EDS analysis of CoNC.

Element	Weight%	Atomic%
C K	43.95	67.21
N K	11.25	14.75
O K	4.88	5.6
Co L	39.91	12.44
Totals	100	

Table 4.4 SEM-EDS analysis of Pd/CoNC.

Element	Weight%	Atomic%
C K	44.29	70.76
O K	10.74	12.88
Cl K	11.60	6.28
Co L	27.93	9.09
Pd L	5.44	0.98
Totals	100	

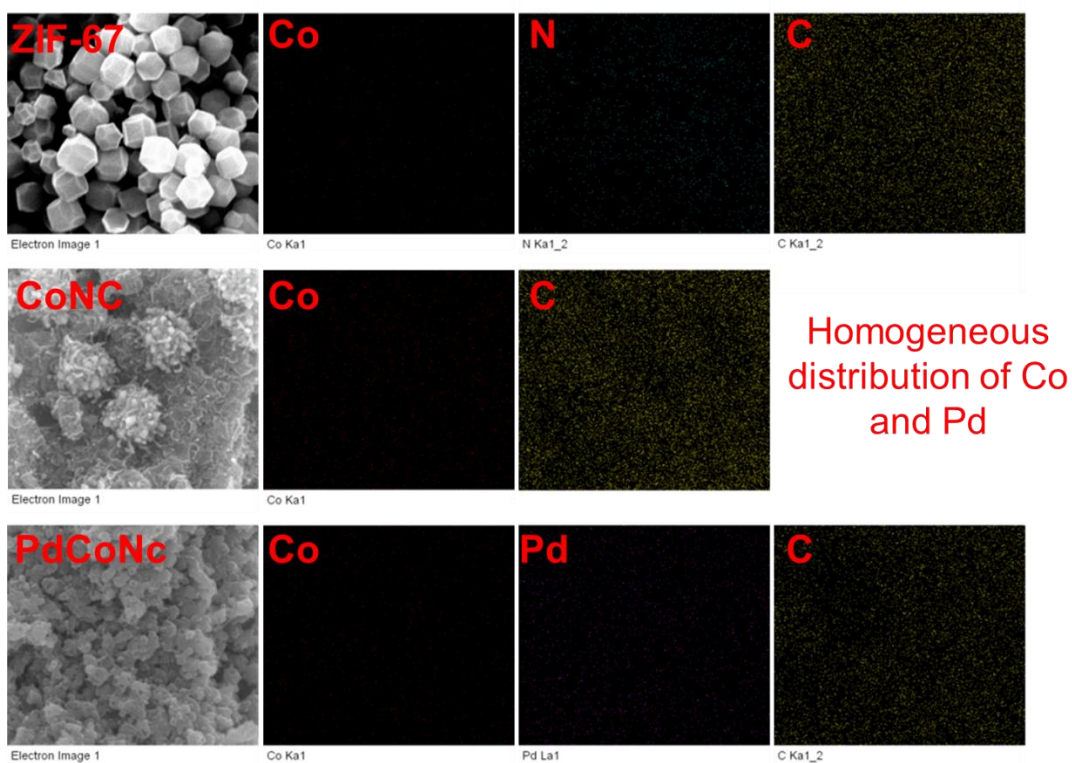
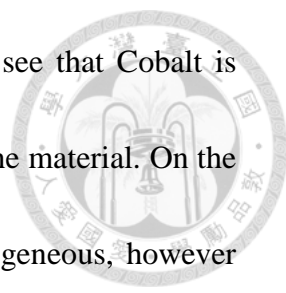


Figure 4.8 SEM-EDS mapping images showing homogeneous distribution of Co and Pd on the material.



As seen from the SEM-EDS analysis and mapping, we can see that Cobalt is homogeneously distributed and the wt% of Cobalt is also high on the material. On the other hand, the distribution of palladium on the material is homogeneous, however from the SEM-EDS analysis, the content of palladium is significantly lower than what we have expected. This could be due to the difficult operation of the incipient wetness impregnation. Increasing the number of impregnations or lowering the acidity of the precursor solution could remedy this problem.

4.5.2. Transmission electron microscopy (TEM)

The ZIF-67, CoNC and Pd/CoNC samples were sent to NIMS, Japan for analysis of the structure and electron diffraction of the materials. The samples were analyzed with a JEM-2010 TEM system operated at 200 kV.

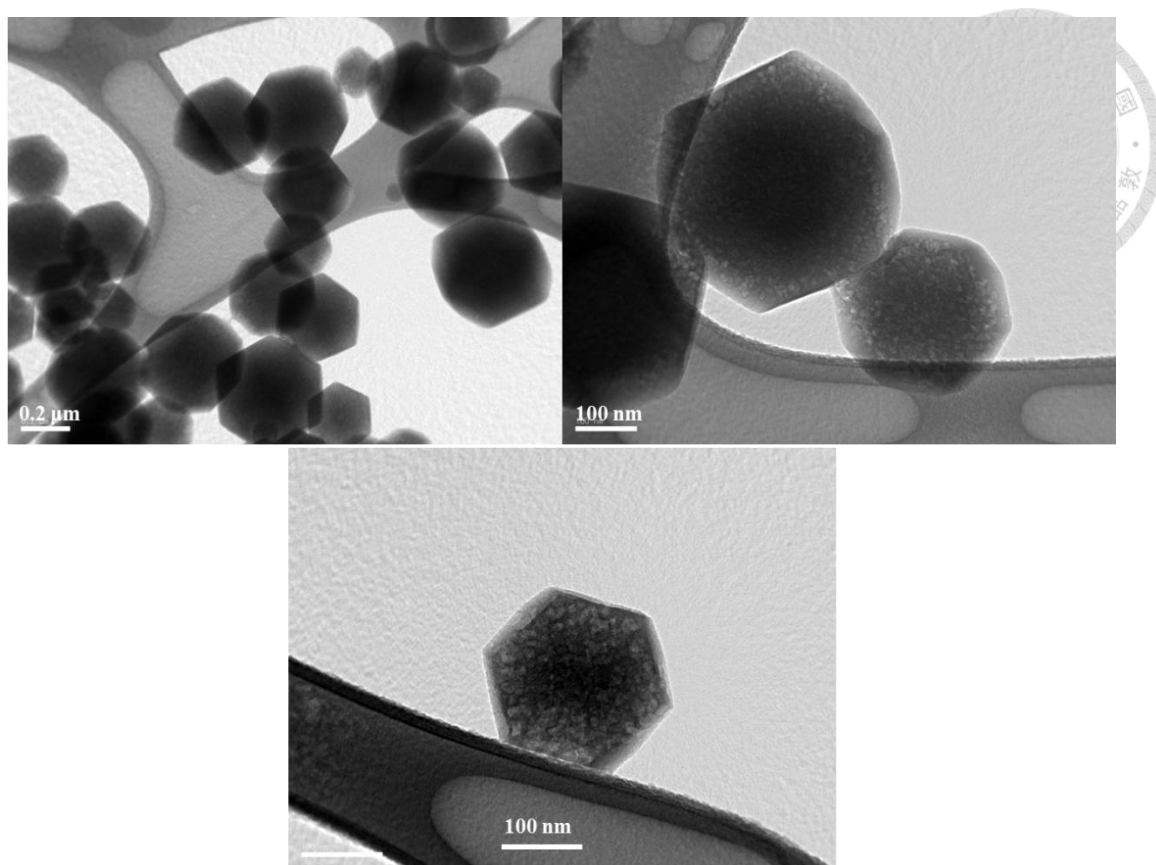


Figure 4.9 ZIF-67 TEM images through different magnifications.

As can be observed from the Figure 4.9, the particle sizes of ZIF-67 were about 300 nm in average. Rhombic dodecahedral shapes were also observed. From Figure 4.10, there is a homogeneous distribution of Cobalt on CoNC, Cobalt can be observed as darker dots inside the large particle. As seen in Figure 4.11, CoNC contains polycrystallinity, shown as circles surrounding a center.

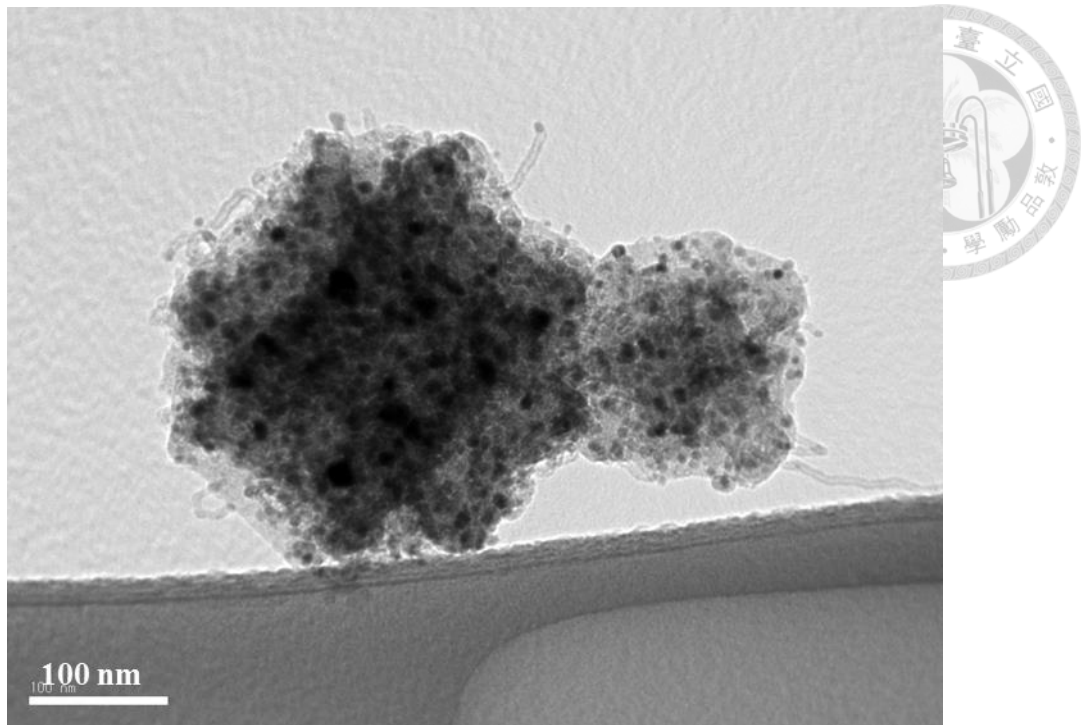


Figure 4.10 TEM image of CoNC.

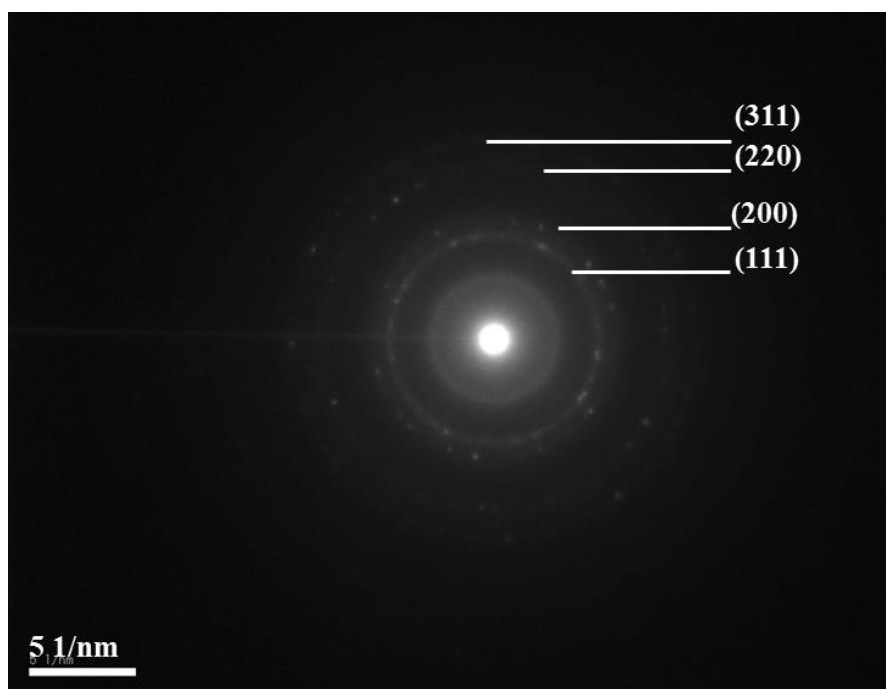


Figure 4.11 TEM Selected-area electron diffraction patterns of CoNC.

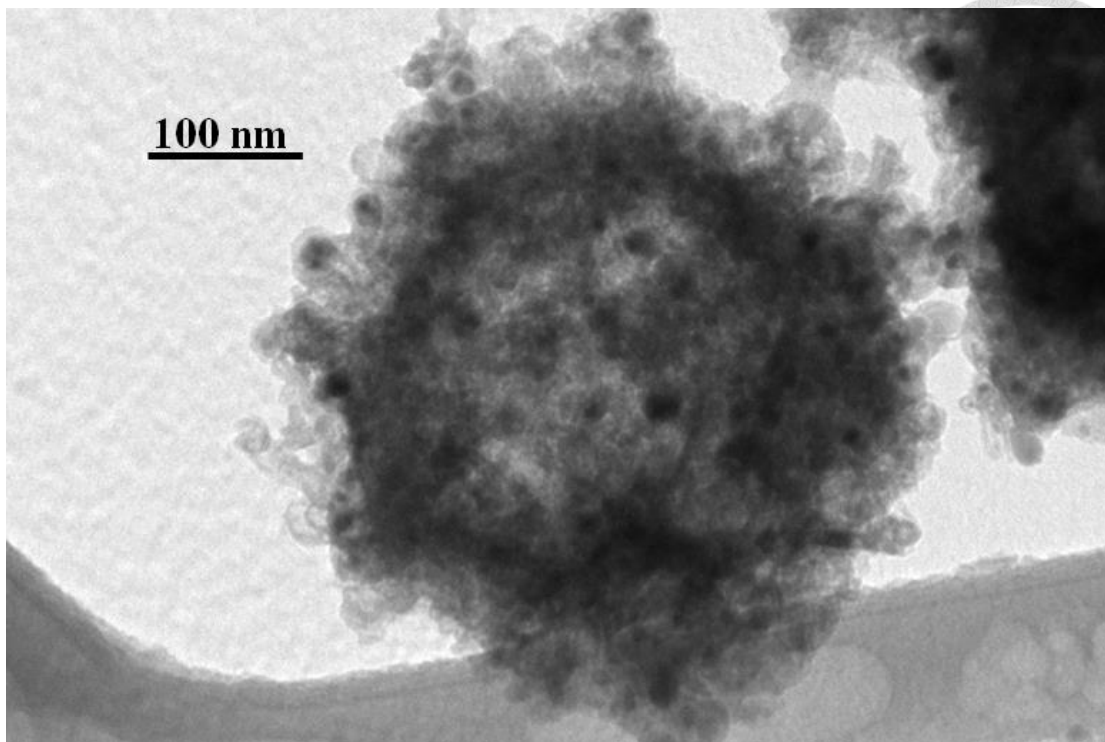


Figure 4.12 TEM image of Pd/CoNC.

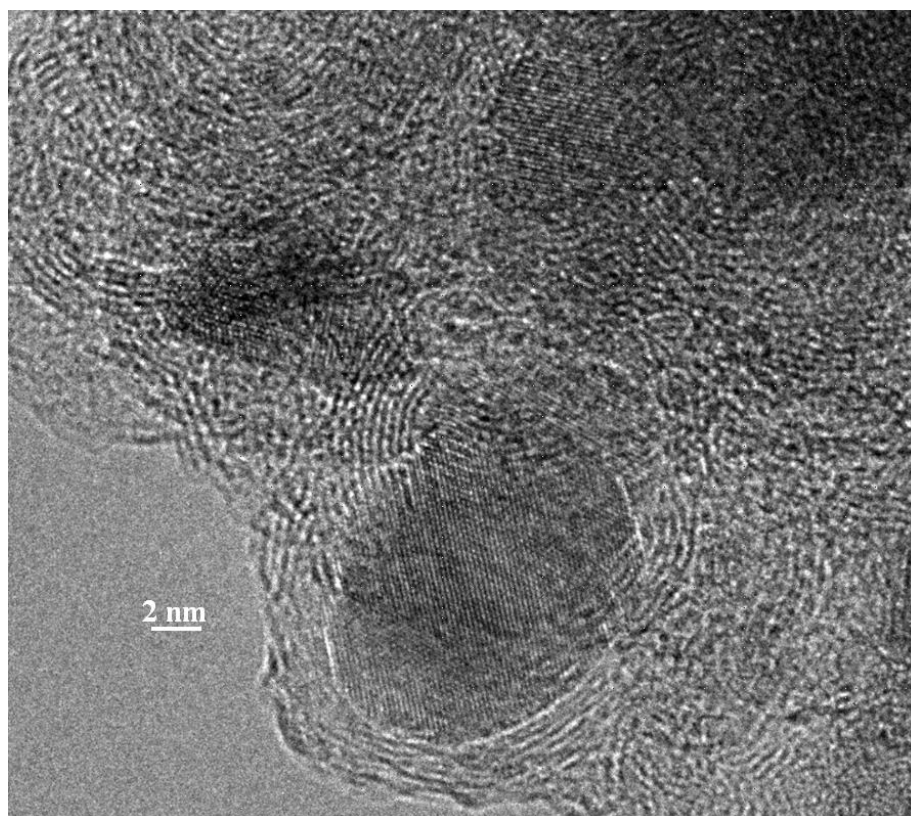


Figure 4.13 Pd/CoNC with Cobalt and Palladium Particles shown.

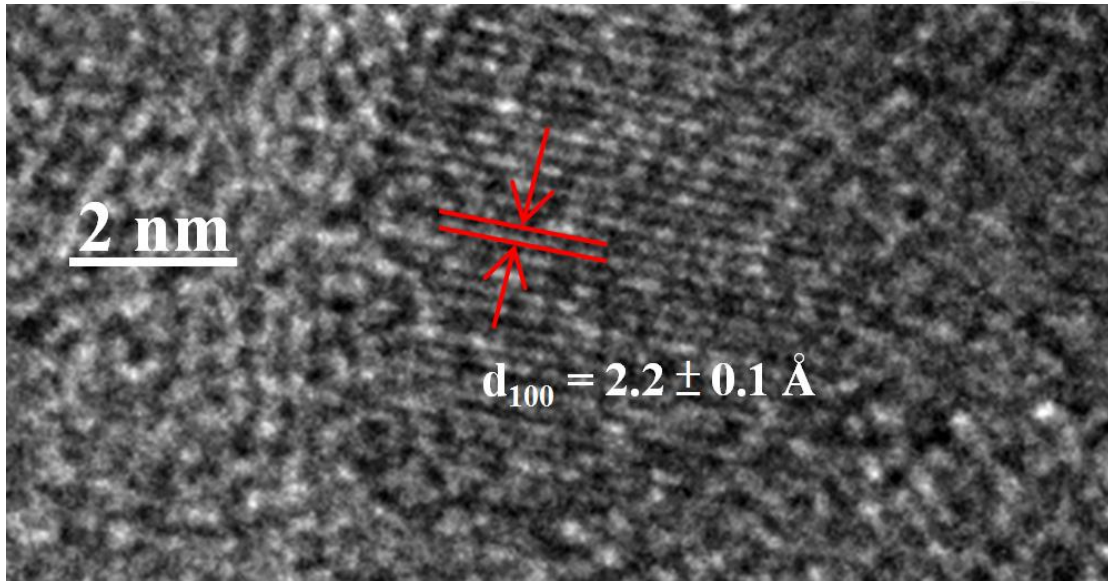


Figure 4.14 Focused TEM image on Cobalt particle.

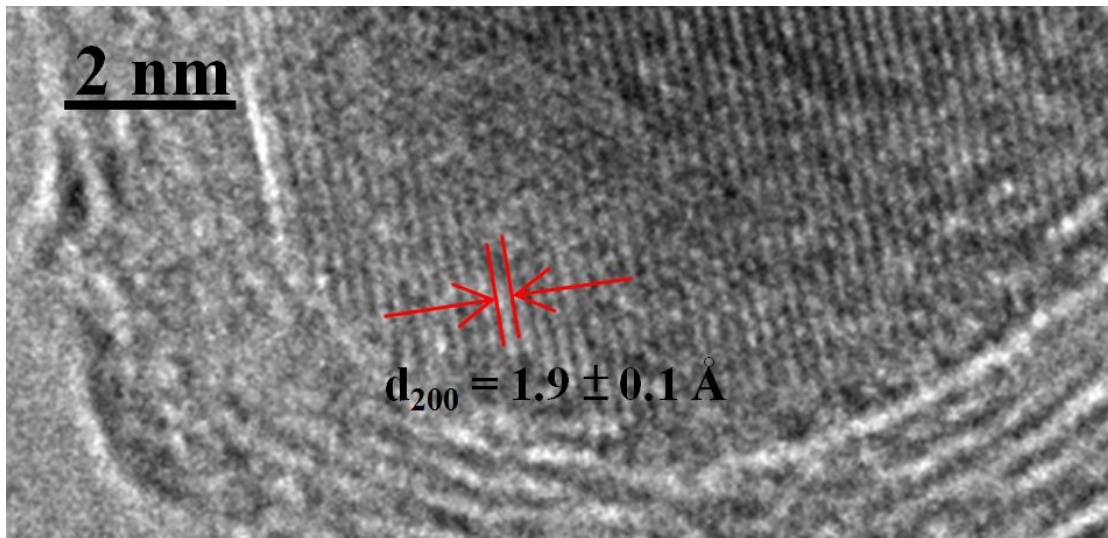


Figure 4.15 Focused TEM image on Palladium particle.

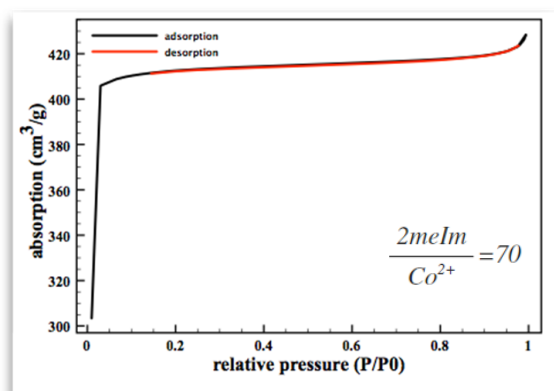
From the TEM images of Pd/CoNC, it is observed that a single Pd/CoNC particle is about 300 to 400 nm in size, and it contains a homogeneous distribution of Palladium and Cobalt inside the particle. The Palladium and Cobalt particles are very

small in size, at 6 nm maximum.



4.5.3. Specific Surface Area Analyzer

The nitrogen adsorption/desorption isotherm was measured with Micromeritics ASAP 2010. The specific surface area was evaluated correspondingly. Samples were dehydrated at 100°C to avoid misevaluating the dried weight. After cooling to room temperature, the samples were analyzed under 77K.



- **Specific Surface Area: 1804.3 m²/g**
- **Micropore Area: 1321.4 m²/g**
(73.2% of Total)
- **Avg. Pore Diameter: 1.9 nm**

Figure 4.16 N₂ adsorption/desorption isotherm of ZIF-67.

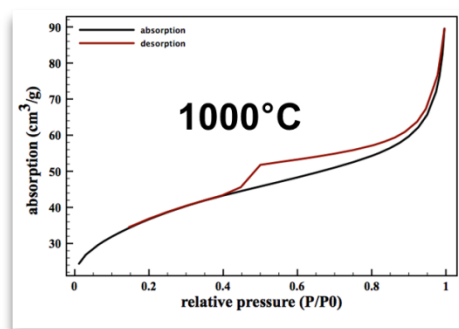
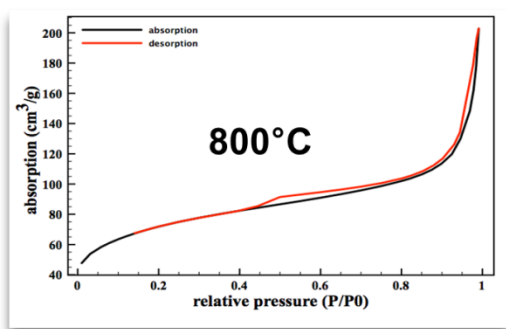
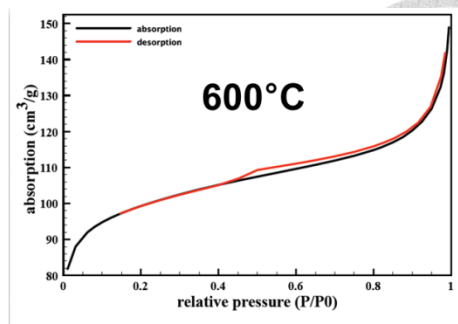
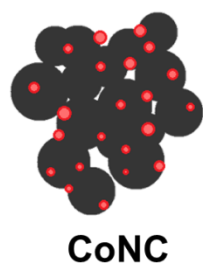
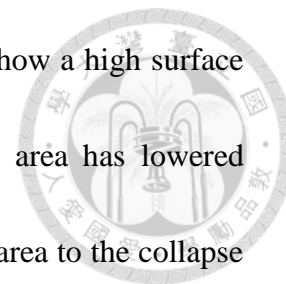


Figure 4.17 N₂ adsorption/desorption isotherm of CoNC.

Table 4.5 CoNC under different calcinations temperatures.

Carbonization Temperature (°C)	Specific Surface Area (m²/g)	Micropore Area (m²/g)	Micropore Area %
600	448.56	238.4	53.1
800	347.08	78	22.5
1000	180.09	25.6	14.2

From the surface area analysis we can see that ZIF-67 does show a high surface area of 1800 m²/g, however after the carbonization, the surface area has lowered significantly and from SEM images, we can relate the low surface area to the collapse of the network. Choosing the highest surface area, a carbonization temperature of 600°C was chosen.



4.5.4. X-Ray Diffraction (XRD)

Wide-angle patterns of powder X-ray diffraction (XRD) were measured on Rigaku Ultima IV with Cu K α radiation ($\lambda=1.5418$ Å) to check the crystallinity.

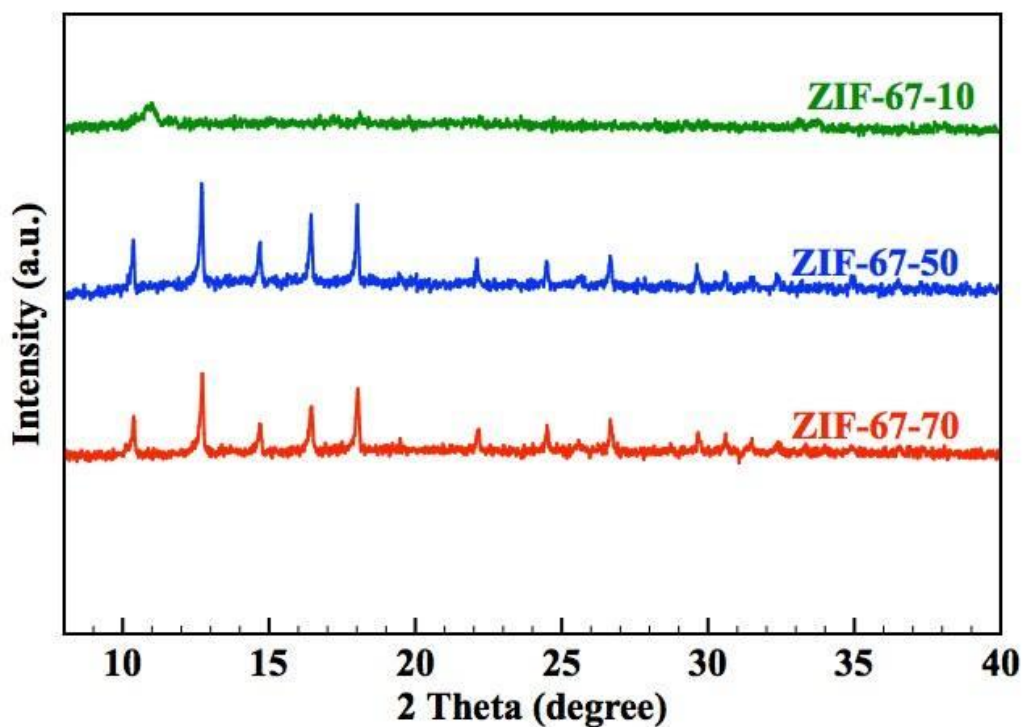


Figure 4.18 XRD pattern of ZIF-67 under different precursor ratios.

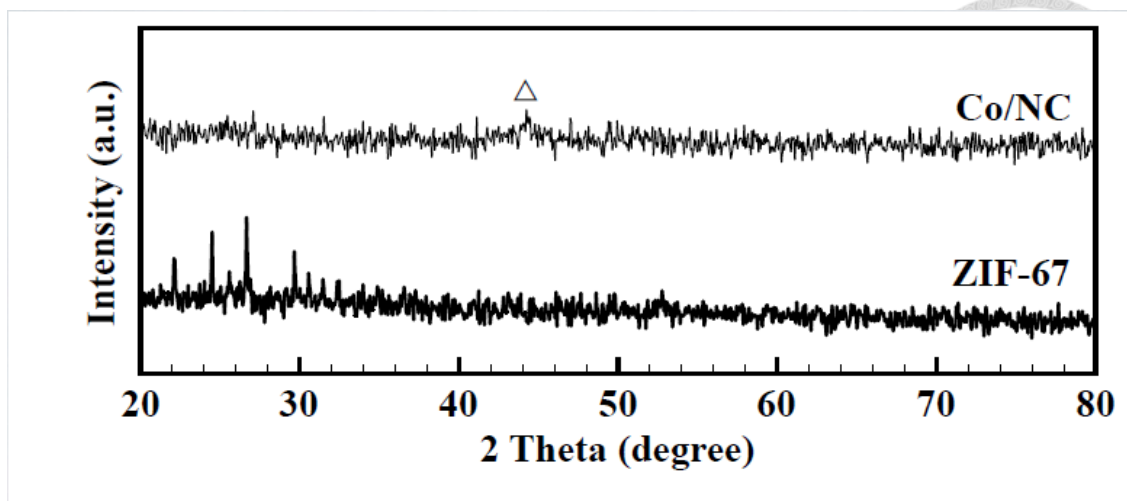


Figure 4.19 XRD pattern of ZIF-67 and CoNC.

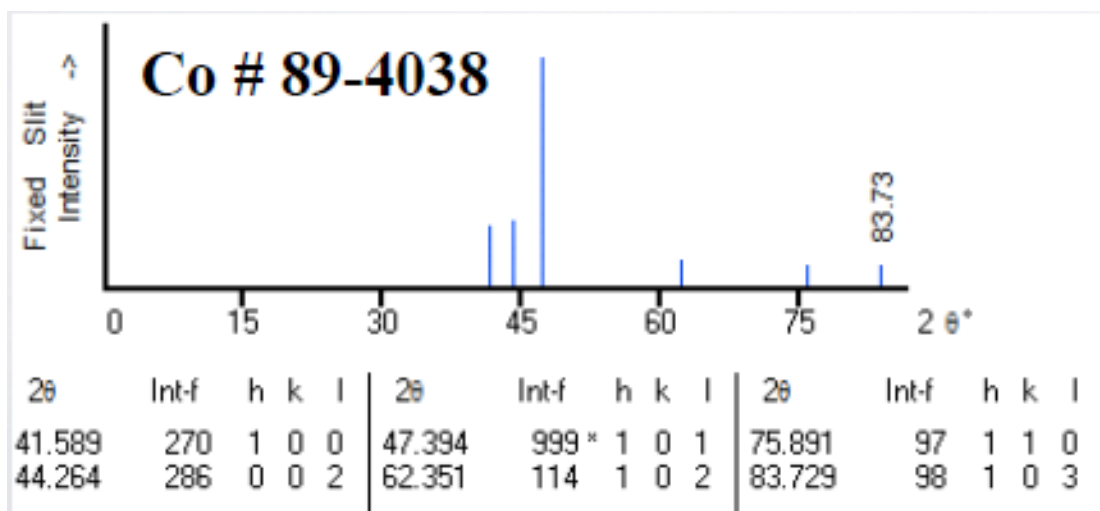


Figure 4.20 Standard XRD pattern of Cobalt.

From the XRD analysis, we can see from Figure 4.10 that a precursor ratio of 10 produces amorphous ZIF-67. Figure 4.11 shows the XRD analysis of CoNC, where a standard of Cobalt shows that there is in fact slight appearance Cobalt. The broad peak could be attributed to the small particle size according to Scherrer's equation.

However from Figure 4.13, the material shows magnetic properties, meaning there is metal content in the material, which could only be Cobalt.



Figure 4.21 Magnetism demonstrated in CoNC.

4.5.5. Thermogravimetric Analysis

The program for the thermogravimetric analysis was done under an increasing temperature range of 30°C ~800°C with a temperature increase rate of 5°C/min.

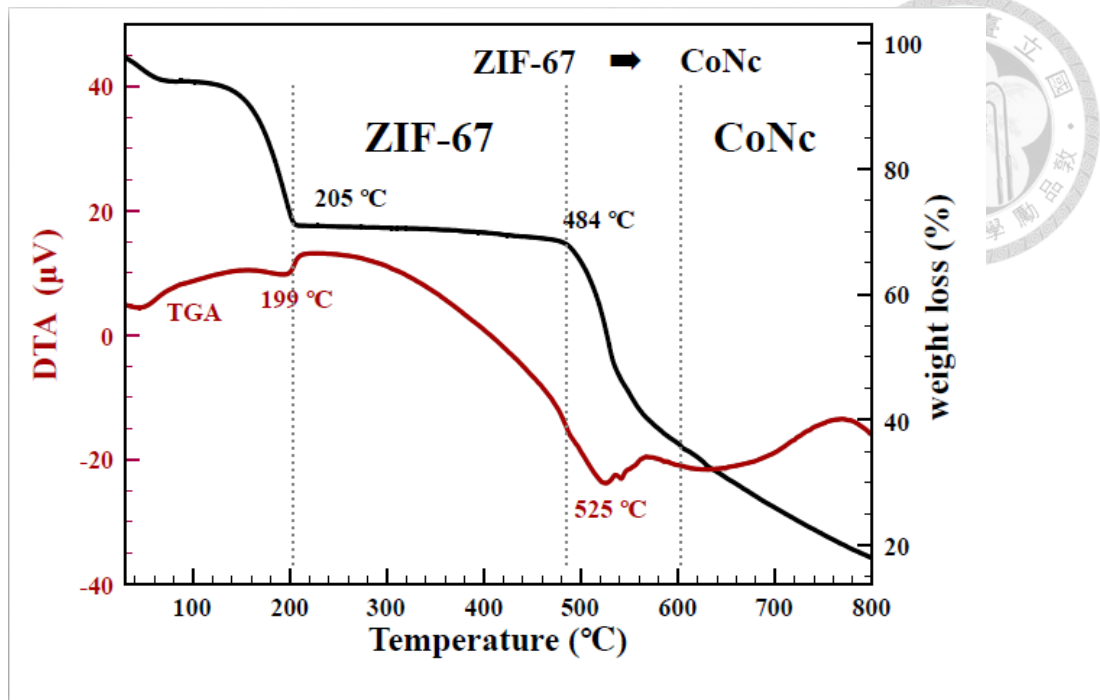


Figure 4.22 Weight loss profile of ZIF-67 to CoNC conversion.

From the weight loss, we can see that a calcination temperature of 600°C converts most of the ZIF-67 particles into CoNC particles. Even though temperatures higher than 600°C continue to convert the particles into CoNC, it was shown previously that higher calcination temperatures decrease the surface area of the material.

4.5.6. Calibration Curve for DMF

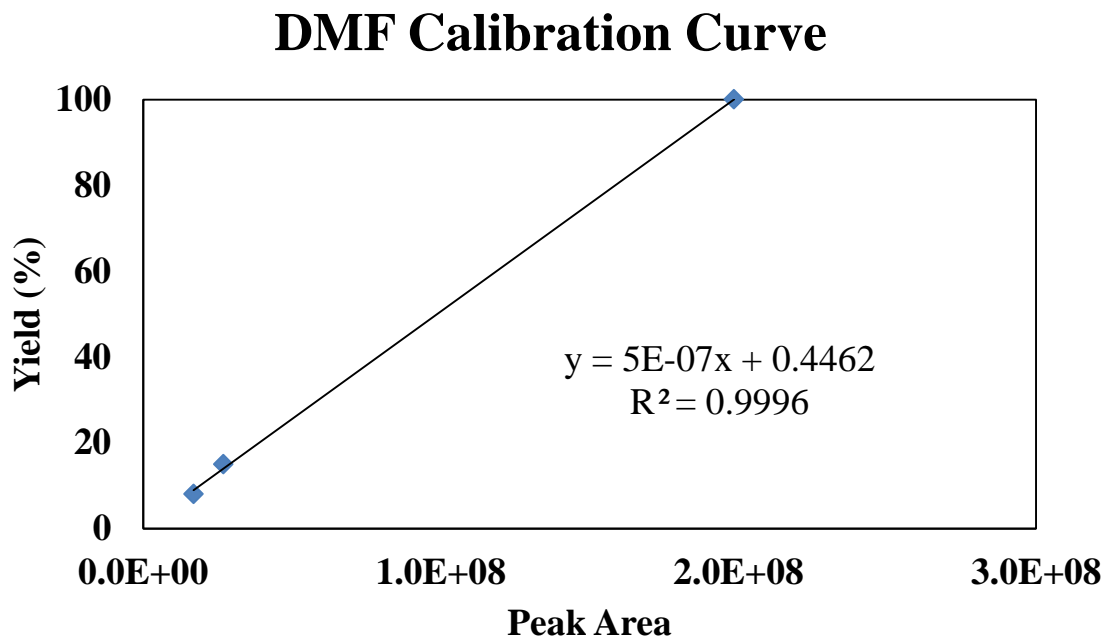


Figure 4.23 Calibration Curve for DMF.

4.5.7. Calibration Curve for MFAD

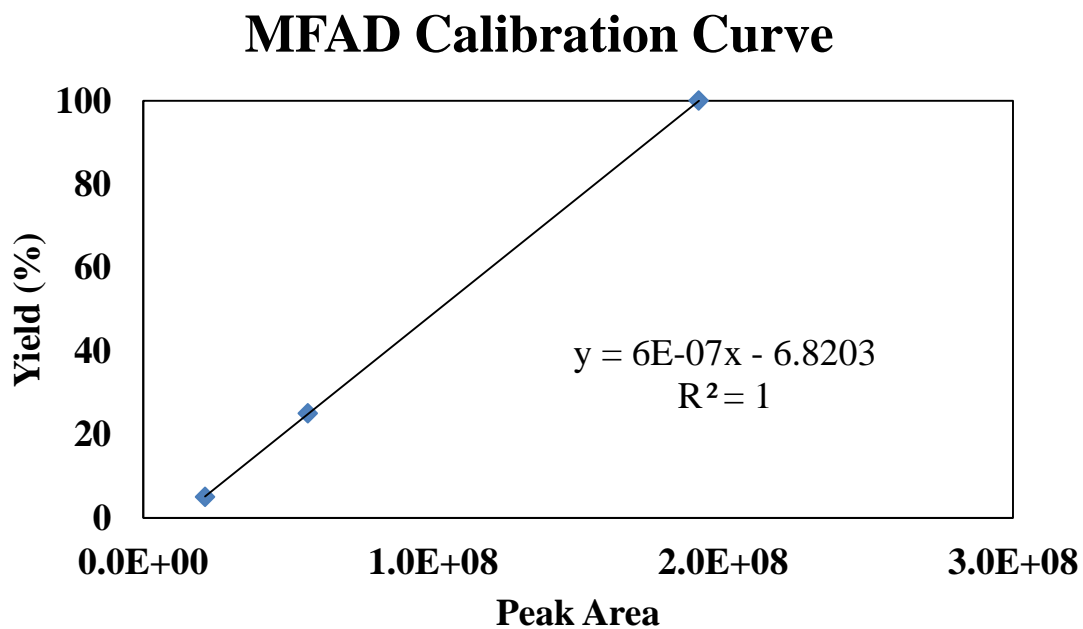


Figure 4.24 Calibration Curve for MFAD.

5. RESULTS and DISCUSSION



5.1. HMF as the starting reactant

The experiment uses HMF as a starting reactant because it is a well-known chemical platform in which most of the DMF synthesis works have been using as a starting reactant.

5.1.1. Effect of Catalyst Amount

It can be seen below in Figure 5.1 that 0.1 g of catalyst proves to be the most efficient amount as increasing the amount to 0.15 g decreases the yield. Although some may argue that increasing the catalyst amount further would enhance the catalytic activity, having a balanced reactant to catalyst ratio would be more important in understanding the capabilities of a catalyst. Although some may argue that there may be errors involved in these tests, running more trials on these tests may seem trivial since none of the yields exceed 10%.

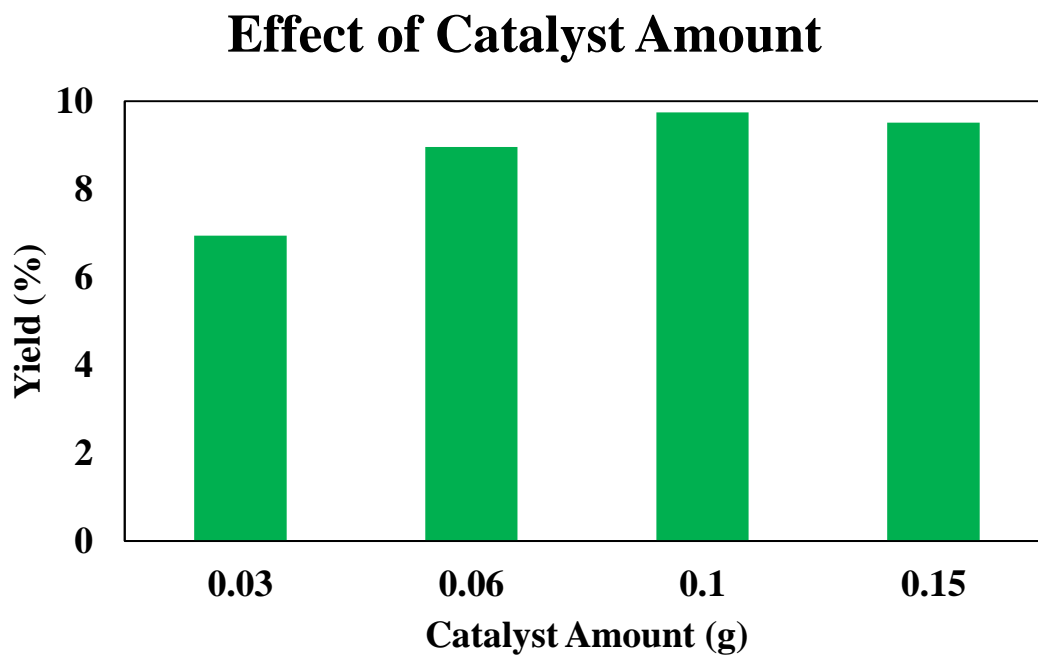


Figure 5.1 Yield of DMF varying catalyst amounts. 4.5 mL THF in 7 mL

Vial, 0.05 g HMF, 0.06 g NaBH₄, 1 mL DI Water, 303K.

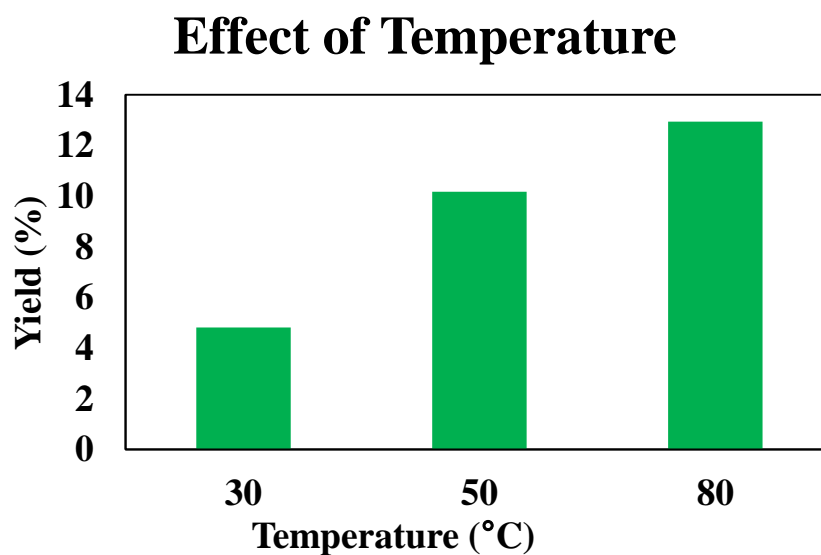


Figure 5.2 Yield of DMF varying reaction temperatures. 4.5 mL THF in

10 mL Vial, 0.05 g HMF, 0.06 g NaBH₄, 1 mL DI Water, 0.1 g Catalyst.

5.1.2. Effect of Reaction Temperature

As shown in Figure 5.2, 353K proves to be the most suitable for the synthesis of DMF. Going against the goals of this research, temperature variables were still tested because yields would not exceed 15% at this point. Since most of the other works have conducted this reaction under higher temperatures, it was guessed that maybe temperature was the key to this reaction. After these tests, it was proven that temperature does effect the yield of this reaction, but the key to a massive increase of the yield for this reaction lies somewhere else.

5.1.3. Effect of Reaction Time

The results shown in Figure 5.3 suggest that a notable increase of DMF yield occurs at 3 hours. Figure 5.3 and 5.4 are conducted under different reaction containers. Figure 5.4 shows higher yield due to the suspected higher pressure related with the smaller amount of reactor volume. Nonetheless, it can be concluded that even after 9 hours, the yield of DMF remains at about 10%, meaning 3 hours is the optimum reaction time. It is also favored to have a shorter reaction time.

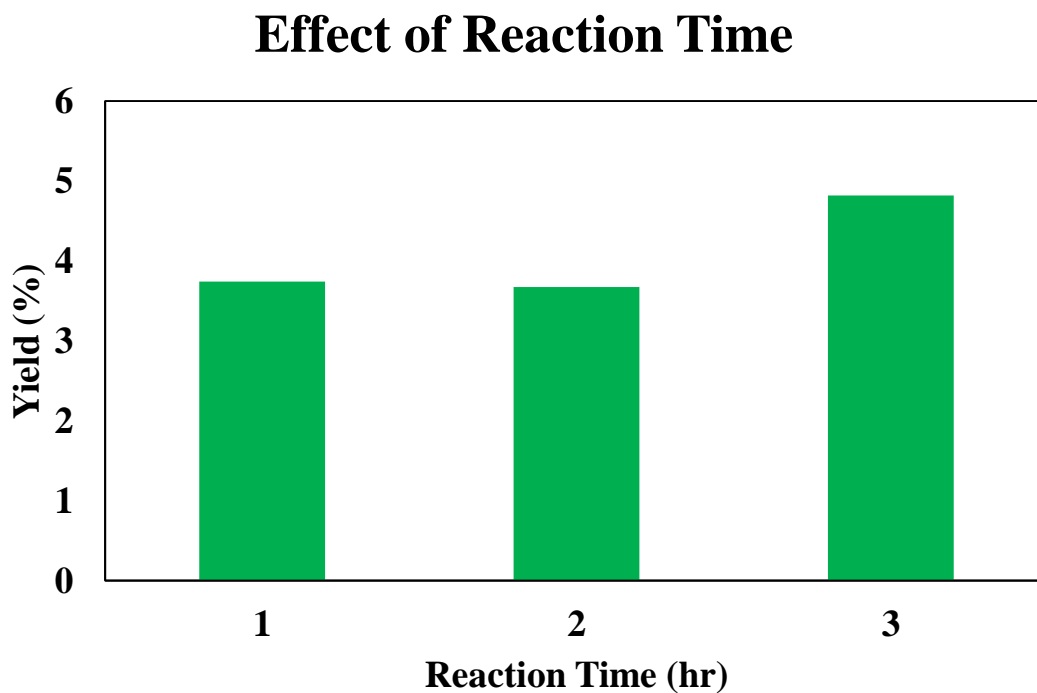


Figure 5.3 DMF yield varying reaction time. 4.5 mL THF in 10 mL Vial,
0.05 g HMF, 0.06 g NaBH₄, 1 mL DI Water, 0.1 g Catalyst.

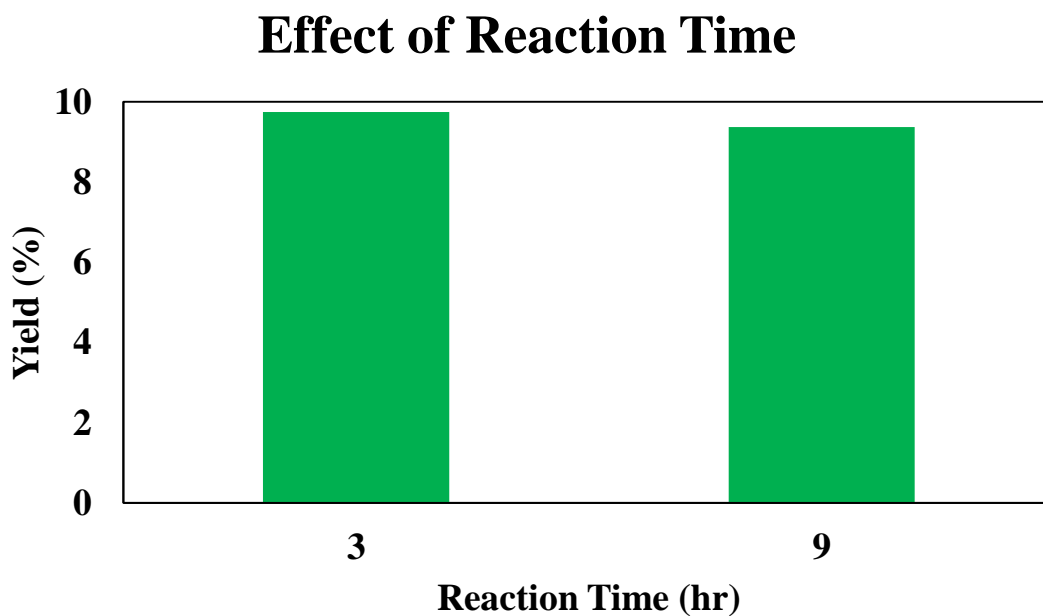
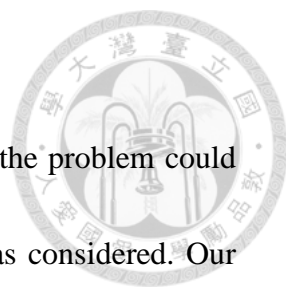


Figure 5.4 DMF yield varying reaction time. 4.5 mL THF in 7 mL Vial,
0.05 g HMF, 0.06 g NaBH₄, 1 mL DI Water, 0.1 g Catalyst.

5.1.4. Effect of NaOH addition



After trying out several obvious and easily tunable variables, the problem could be confirmed to be elsewhere, therefore the addition of NaOH was considered. Our source of hydrogen comes from NaBH_4 , and the rate of hydrogen production is determined by the acidity of solution it is dissolved in. Solutions of higher acidity will increase the rate of hydrogen production while lower acidity will decrease the production rate. The high hydrogen production rate could lead to unused hydrogen gas that would rise to the top of the reactor due to the low solubility of hydrogen gas in most solvents. When the hydrogenation rate is significantly lower than the hydrogen production rate, there would be less contact between hydrogen gas and the active site. Therefore it is thought that a slower hydrogen production rate will help achieve a steady state of hydrogen usage and production. It could be argued that increasing the amount of NaBH_4 would lead to the same result, but it would be most efficient if the least NaBH_4 could be used. It can be seen on Figure 5.5 that addition of NaOH does indeed slow down the production of hydrogen, which leads to lower yields under 3 hours of reaction. Temperature varying tests were also given to show that even under reaction at 353K, DMF yield could not exceed that of reactions without NaOH additions.

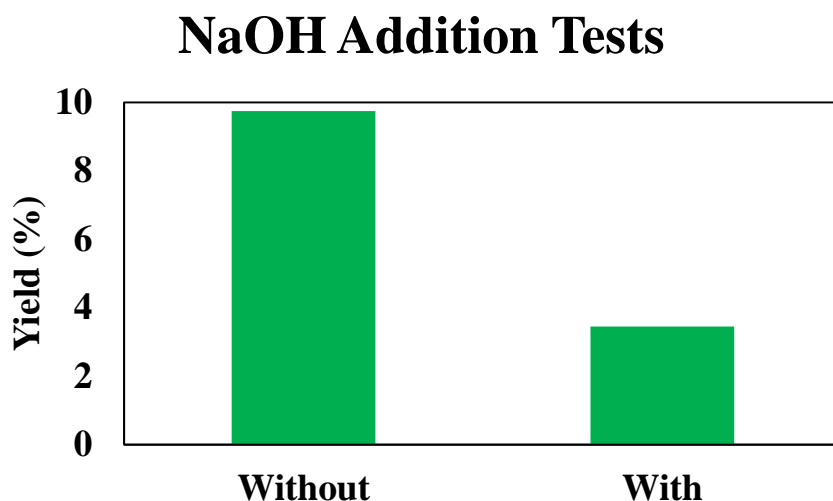


Figure 5.5 DMF yield with or without NaOH addition. 4.5 mL THF in 7 mL Vial, 0.05 g HMF, 0.06 g NaBH₄, 0.14 mL DI Water + NaOH, 0.1 g Catalyst, 3 hr.

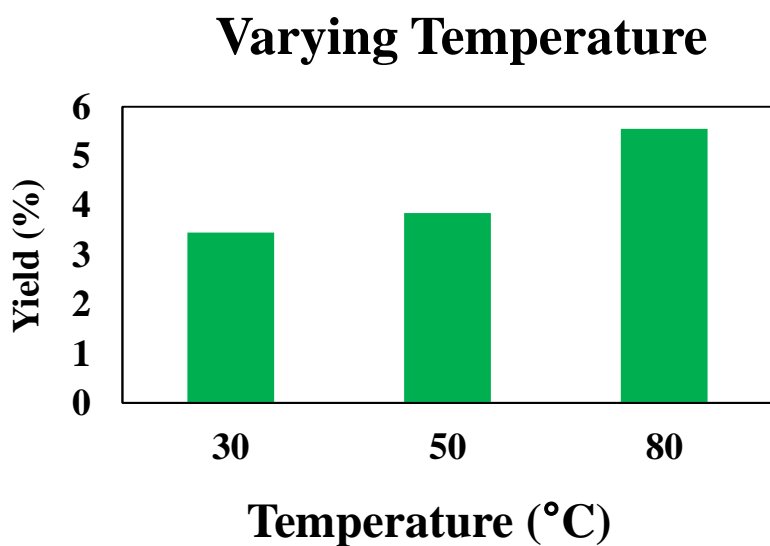
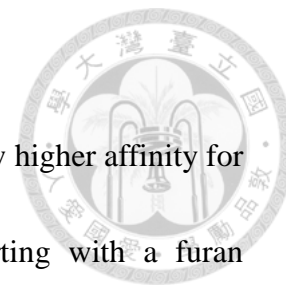


Figure 5.6 DMF yield with NaOH addition varying temperature. 4.5 mL THF in 7 mL Vial, 0.05 g HMF, 0.06 g NaBH₄, 0.14 mL DI Water + NaOH, 0.1 g Catalyst, 3 hr.

5.2. Comparison of Different Starting Reactants



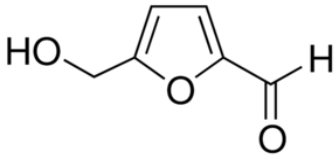
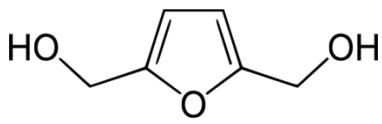
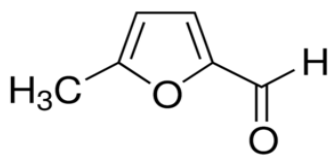
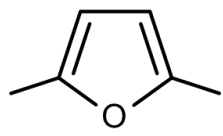
With knowledge that supported palladium catalysts often show higher affinity for aromatic aldehyde substituents, it was then proposed that starting with a furan structure that contains only aldehyde groups would amount to a higher yield of DMF. As the aldehyde substituents attach itself on the palladium surface, the hydrogenation of the aldehyde group to an alcohol group occurs, while the hydrogenolysis of the alcohol group instantly follows. This higher affinity between the palladium surface and the aldehyde group compared to the affinity between the palladium surface and an alcohol group could possibly amount to a higher yield of DMF. Two possible candidates were 5-Methylfurfural (MFAD) and 2,5-diformylfuran (DFF). 5-Methylfurfural has a similar structure to HMF, except that the alcohol group on HMF has been replaced with a methyl group. This means that MFAD needs to go through only two reaction steps as compared to three of HMF to be converted into DMF, which means that a higher yield should be anticipated as shown in Table 5.1. One of the major benefits of using MFAD as the starting reactant lies in that it is significantly cheaper than HMF. At this point of research, these results were enough to justify the use of MFAD as the starting reactant for this research. Using DMF as a starting reactant proves that there weren't any further reactions that could occur in this system. As shown in Table 5.1, BHMF having lower DMF yield compared to HMF

supports the idea that our catalyst shows higher affinity for aromatic aldehyde groups

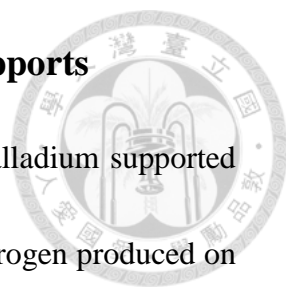
compared to aromatic alcohol groups.



Table 5.1 Yield of DMF starting from different reactants.

Reactant	DMF Yield (%)
HMF 	4.8
BHMF 	3.7
MFAD 	7.4
DMF 	100

5.3. Palladium and Cobalt on Same or Different Supports



It was proposed in this thesis that the effect of Cobalt and Palladium supported on the same support would create a synergetic effect where the hydrogen produced on the cobalt would immediately be adsorbed by the palladium surface to conduct hydrogenation reactions, therefore tests on palladium and cobalt on different supports were conducted. It can be seen from Figure 5.7 that when Palladium and Cobalt are supported on the same supports, they do exhibit synergetic effects to give higher yield. It could be because when Cobalt and Palladium are supported on different supports, the distance increases between these sites, so the hydrogen produced won't be adsorbed by the Palladium surfaces, therefore it floats to the liquid surface before utilization.

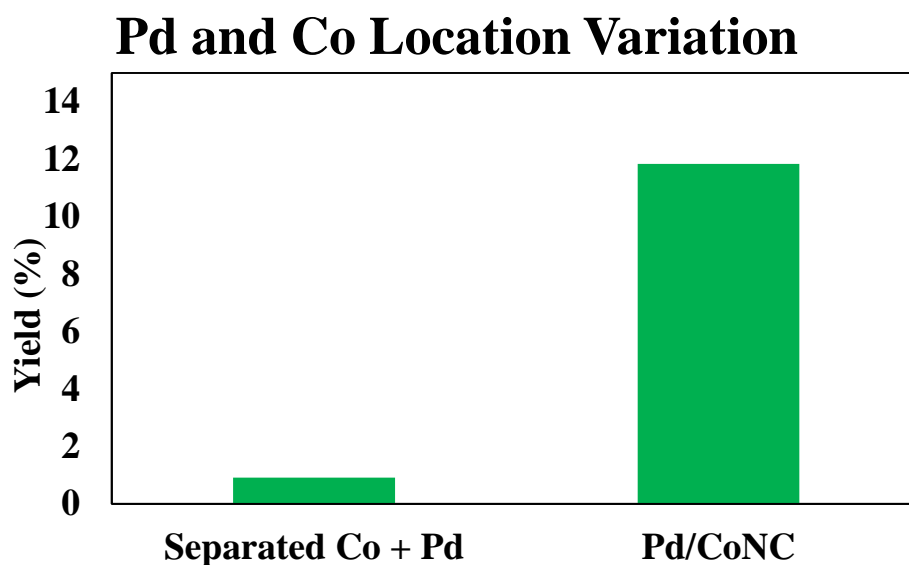


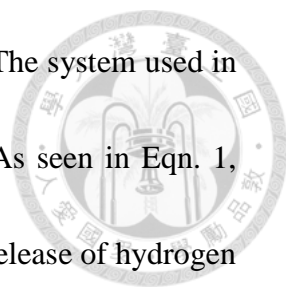
Figure 5.7 DMF yield with Pd and Co location variation. 4.5 mL THF in 7 mL Vial, 0.05 g HMF, 0.06 g NaBH₄, 1 mL DI Water, 303K.

5.4. Reactions Starting with MFAD

As MFAD has been proven to be more efficient in terms yield and it is significantly cheaper than HMF (With MFAD being 3.96 US dollars per gram and HMF being 27.6 US dollars per gram on the Sigma Aldrich website as of June 11th, 2014), the following experiments have been conducted with MFAD as the starting reactant.

5.4.1. With or Without Acid Addition

As the research progressed, most of the variables have been tried. After a comparison with other works on DMF synthesis, it was found that most of the other



works have been based on either acidic or neutral environments.⁵² The system used in this research would become more basic as the reaction went on. As seen in Eqn. 1, sodium borohydride is converted into sodium metaborate after the release of hydrogen gas, and sodium metaborate is a basic compound. Therefore, externally added acid is needed to bring the reaction environment to neutral or acidic conditions. Sulfuric acid was chosen for this work because HCl could have leaching effects on our catalyst due to the tendency of Cobalt forming Cobalt chloride. It was mentioned in the experimental section that two different systems were explored in this experiment, because the timing for the addition of sodium borohydride could be crucial for determining the environment of the reaction. Therefore it can be seen in Figure 5.8 and 5.9 that the addition of acids together with sodium borohydride would negate the acid effect too soon which means the solution turns basic too soon. The slow addition of sodium borohydride results in the solution being acidic for a longer period of time, resulting in higher yields. It can be seen on Figure 5.10 that the addition of acid does in fact increase the yield significantly. Therefore it is important to find the optimum amount of acid needed. Figure 5.11 shows tests on the optimum amount of sulfuric acid needed for the highest yield.

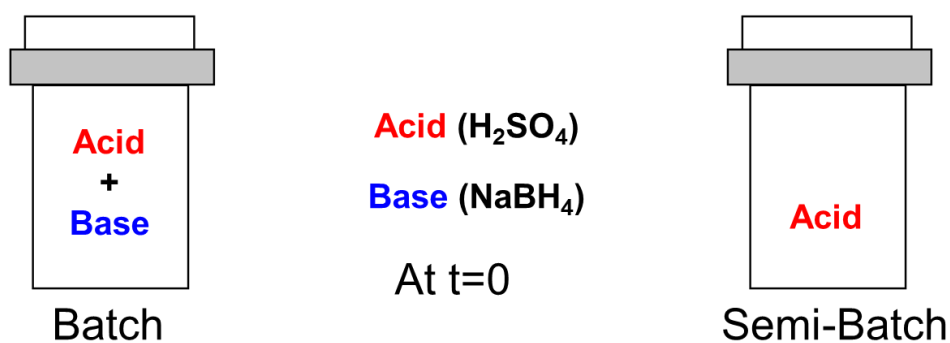


Figure 5.8 Scheme for batch and semi-batch reactions determining the timing for the addition of sodium borohydride.

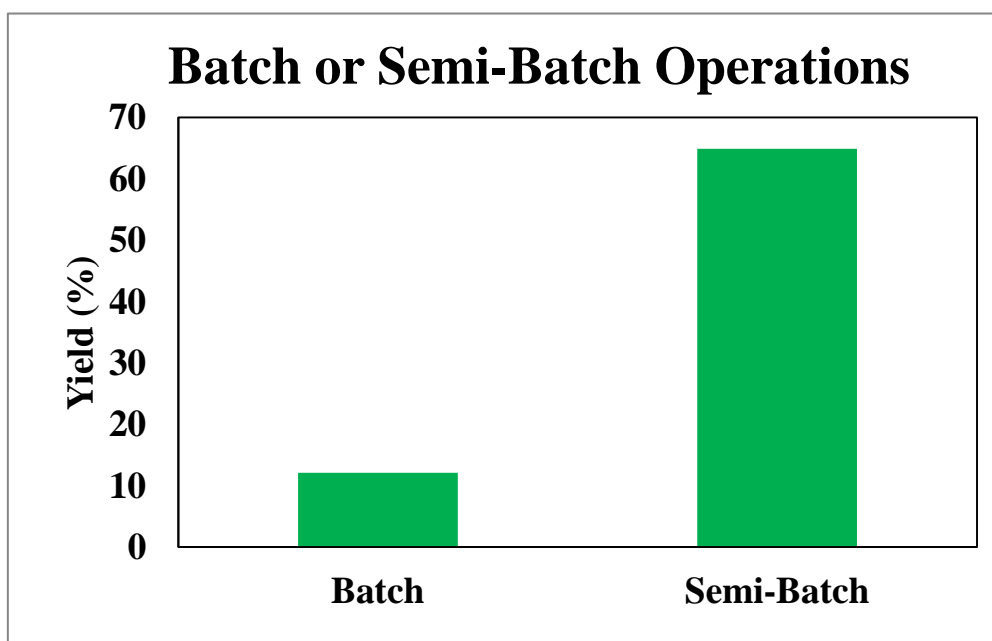


Figure 5.9 Comparison of Batch or Semi-Batch yields.

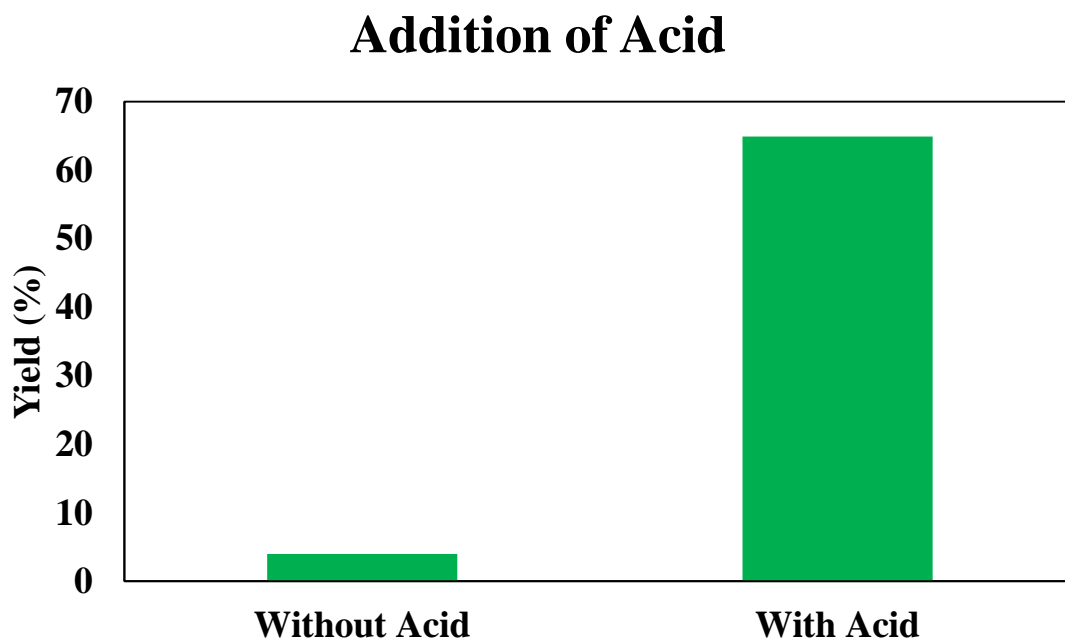


Figure 5.10 DMF yield with or without H₂SO₄ addition. 4.5 mL THF in 20 mL Vial, 39 μL MFAD, 0.06 g NaBH₄, 30 wt% NaOH solution in pump, 0.1 g Catalyst, 303K, 0.34 mL/hr for 3 hr, then 1 hr reaction time.

(8 μL H₂SO₄ added if required.)

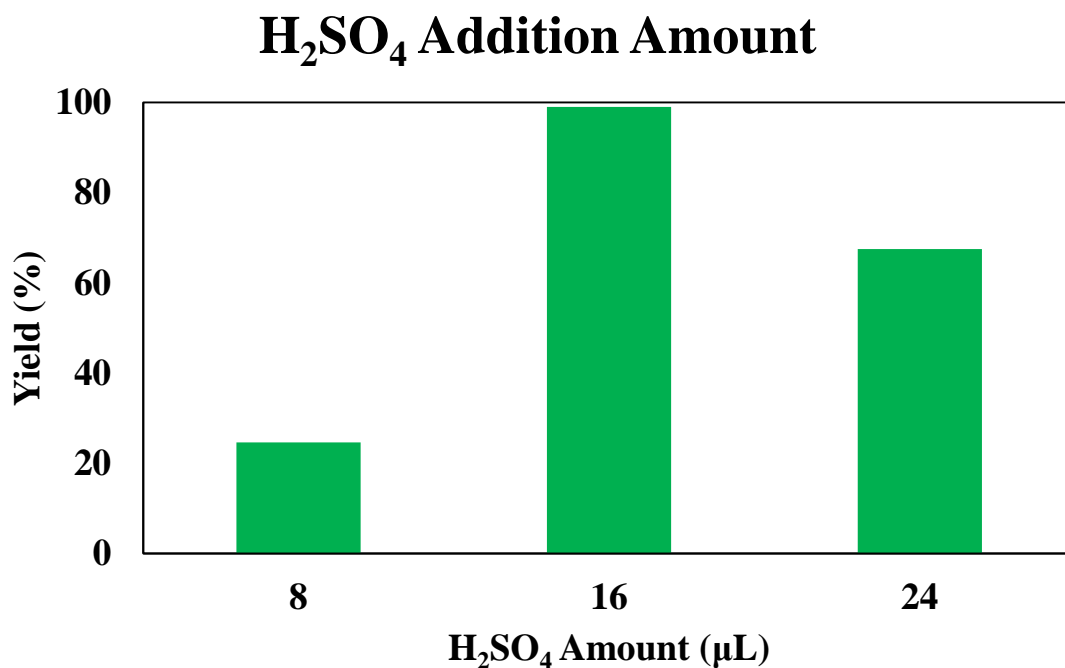
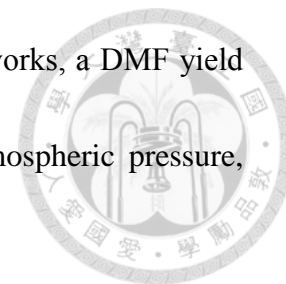


Figure 5.11 DMF yield with addition of varying amounts of H₂SO₄. 4.5 mL THF in 10 mL Vial, 39 µL MFAD, 0.06 g NaBH₄, 30 wt% NaOH solution in pump, 0.1 g Catalyst, 303K, 0.34 mL/hr for 3 hr, then 1 hr reaction time.

5.5. Different Starting Reactants under Optimum Conditions

After the optimum reaction conditions and the right system was found. Tests were done for HMF, DFF and MFAD to confirm once again that the Pd/CoNC catalyst shows higher affinity for aldehyde groups. As seen from the results in Figure 5.12, HMF and DFF shows similar yields, meaning that the yield of the four step reaction from DFF shows similar yields to the three step reaction from HMF. However, using DFF as the starting reactant isn't economic due to its high cost as of

now. All in all, using this system to compare with other group's works, a DMF yield of 54% could still be obtained under room temperature and atmospheric pressure, while using an aqueous source of hydrogen.



Varying Reactant

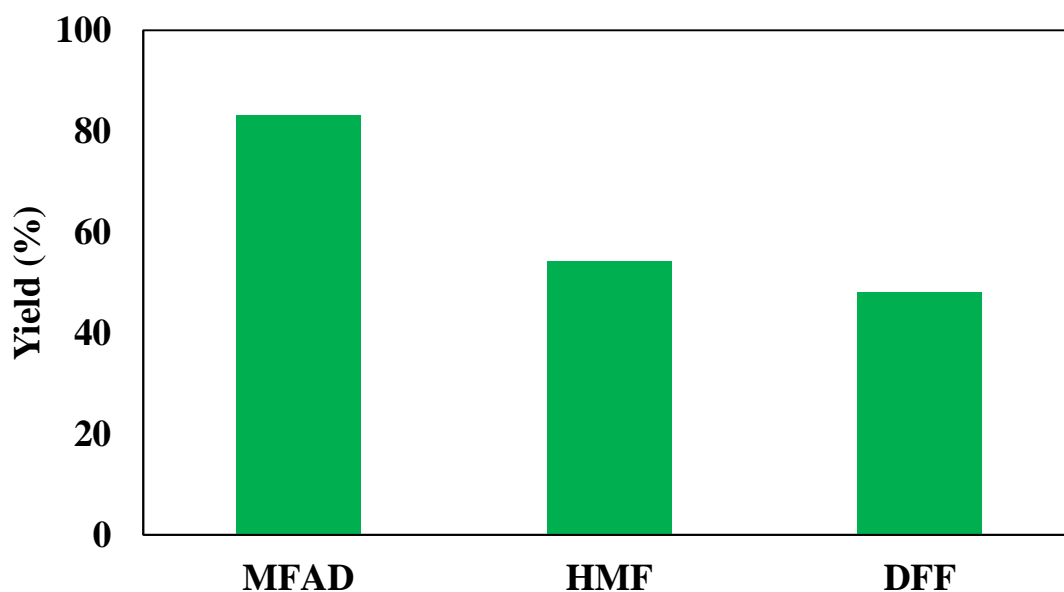


Figure 5.12 DMF yield starting with different reactants. 4.5 mL THF in 10 mL Vial, 0.06 g NaBH₄, 30 wt% NaOH solution in pump, 0.1 g Catalyst, 303K, 1 Atm, 0.34 mL/hr for 3 hr, then 1 hr reaction time.

(Equal mol of Reactant)

5.6. Effect of Atm or Non-Atm Pressure Tests

After the optimum condition was found, tests on atmospheric or non-atmospheric tests were conducted and it can be found that the atmospheric pressure tests result in

better selectivity overall, as shown in the GC-MS spectrums shown in Figure 5.13.

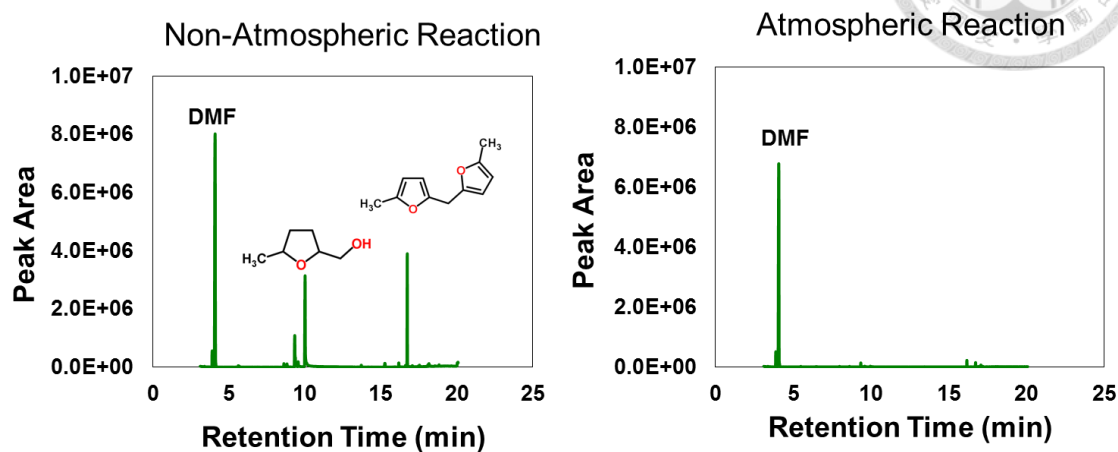


Figure 5.13 Atmospheric and Non-Atmospheric Pressure Tests.

5.7. Synergetic Effects of Cobalt and Palladium

The catalyst effect was tested by going through only using Palladium or Cobalt.

A comparison can be seen in Figure 5.14, where Palladium alone shows poor catalytic effects. It is proposed that it is because Palladium shows no catalytic effects for the production of sodium borohydride, or the competition between the usage of the active site for production of hydrogen or hydrogenation hinders the reaction.

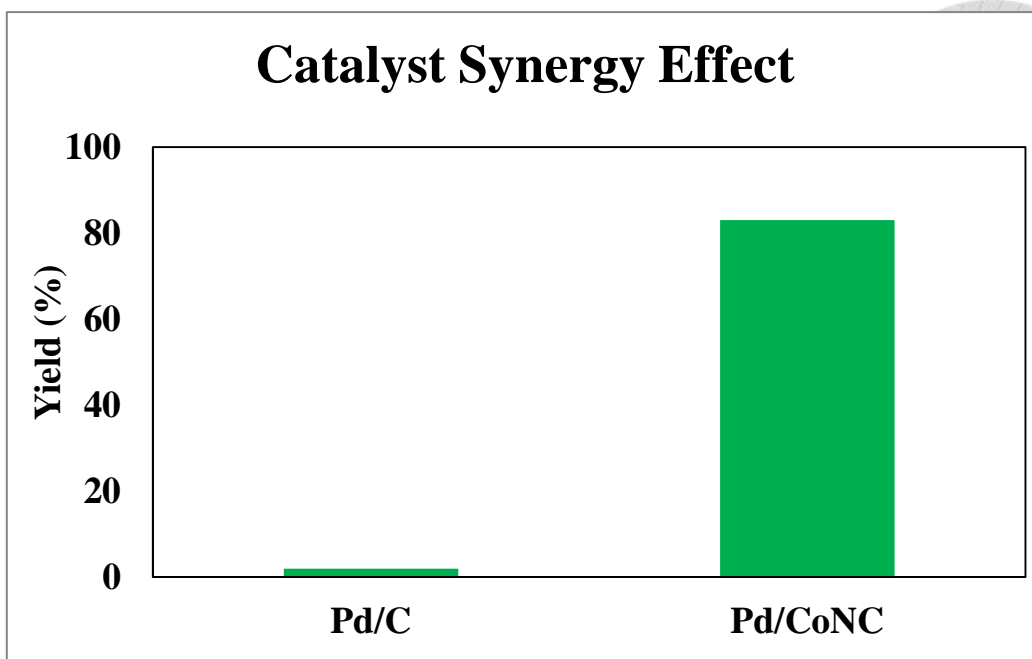


Figure 5.14 Comparison of catalyst with Palladium or Cobalt only.

6. CONCLUSION



In this thesis, we aimed to produce DMF using a novel method never demonstrated before. Using a combination of Sodium Borohydride and our Pd/CoNC catalyst, we were able to provide hydrogen for hydrogenation in the solution under room temperature and atmospheric pressure. The catalyst Pd/CoNC shows bifunctional properties, with Cobalt used as a catalyst for hydrogen production from NaBH_4 and palladium being the catalytic surface for the conversion of reactant to product.

It is also discussed in this thesis that our catalyst shows better affinity for aldehyde groups compared to alcohol groups, and MFAD is significantly cheaper than HMF, which makes it more suitable as a starting reactant when using our catalyst.

The highest yield achieved under room temperature and atmospheric pressure was 83.07% yield of DMF. When using the same starting reactant as other people have used, a yield of 54.1% could still be achieved. We propose that the high yield comes from the fact that hydrogen is produced near the active sites compared to traditional methods where hydrogen is externally added.

7. FUTURE PROSPECTS



As can be seen in the results and discussion section, most of the data were very rough and some of the results did not make sense. This was due to the fact that this work is still in the very early stage of discovery. Most of the experiments were done under the context of an urge to increase the yield.

Going through the whole research again, the catalyst amount could be optimized to have a higher efficiency, while neglecting tests on temperature. The perfect balance between reaction time and the amount of NaOH added could also be tested to obtain the best results. Other homogeneous acids could also be tested to see which of them could show the best effect. Even going further, a catalyst overhaul could be done, such as using other supports like mesoporous silica functionalized with acidic groups to obtain a heterogeneous acid, while depositing palladium and cobalt through methods such as impregnation. This would make even recycling of the catalyst possible, and prevent corrosion of reactor. Catalysts that have never been explored in this field such as ZIF could also be explored. A different hydrogen carrier could also be used, since there have been works using Ammonia Borane (AB) or Hydrazine Borane (HB) as hydrogen carriers and they also produce hydrogen gas rather than providing hydrogen through chemical means (Transfer hydrogenation).^{74,75} Lastly,

recycling tests and different metals could be tried to screen for the best candidate,

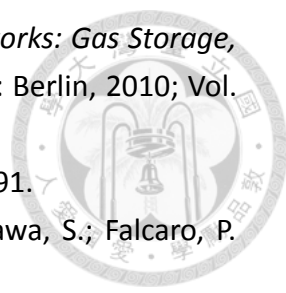
such as replacing precious metals with abundant metals.⁷⁶




8. REFERENCE



- (1) Organisation for Economic Co-operation and Development: <http://www.oecd.org/>.
- (2) International Energy Agency: <http://www.iea.org/>.
- (3) Enerdata: <http://www.enerdata.net/>.
- (4) BP Statistical Review of World Energy: <http://www.bp.com/>.
- (5) Ma, X.; Jiang, C.; Xu, H.; Shuai, S.; Ding, H. *Energy & Fuels* **2013**, *27*, 6212.
- (6) Wu, X.; Li, Q.; Fu, J.; Tang, C.; Huang, Z.; Daniel, R.; Tian, G.; Xu, H. *Fuel* **2012**, *95*, 234.
- (7) Karp, S. G.; Woiciechowski, A. L.; Soccol, V. T.; Soccol, C. R. *Brazilian Archives of Biology and Technology* **2013**, *56*, 679.
- (8) Dutta, S.; De, S.; Saha, B. *Biomass and Bioenergy* **2013**, *55*, 355.
- (9) Sathitsuksanoh, N.; George, A.; Zhang, Y. H. P. *Journal of Chemical Technology & Biotechnology* **2013**, *88*, 169.
- (10) Pereira, A. N.; Mobedshahi, M.; Ladisch, M. R. In *Methods in Enzymology*; Willis A. Wood, S. T. K., Ed.; Academic Press: 1988; Vol. Volume 160, p 26.
- (11) Bergius, F. *Industrial & Engineering Chemistry* **1937**, *29*, 247.
- (12) Mäki-Arvela, P.; Salmi, T.; Holmbom, B.; Willför, S.; Murzin, D. Y. *Chemical Reviews* **2011**, *111*, 5638.
- (13) Sathitsuksanoh, N.; Zhu, Z.; Zhang, Y. H. P. *Cellulose* **2012**, *19*, 1161.
- (14) Moxley, G.; Zhang, Y. H. P. *Energy & Fuels* **2007**, *21*, 3684.
- (15) Zhang, Y. H. P. *Process Biochemistry* **2011**, *46*, 2091.
- (16) LADISCH, M. R.; LADISCH, C. M.; TSAO, G. T. *Science* **1978**, *201*, 743.
- (17) Lee, Y.-C.; Chen, C.-T.; Chiu, Y.-T.; Wu, K. C. W. *ChemCatChem* **2013**, *5*, 2153.
- (18) Karinen, R.; Vilonen, K.; Niemela, M. *Chemsuschem* **2011**, *4*, 1002.
- (19) Wang, T. F.; Nolte, M. W.; Shanks, B. H. *Green Chem* **2014**, *16*, 548.
- (20) Liu, M.; Jia, S. Y.; Li, C. Z.; Zhang, A. F.; Song, C. S.; Guo, X. W. *Chin. J. Catal.* **2014**, *35*, 723.
- (21) Hu, L.; Wu, Z.; Xu, J. X.; Sun, Y.; Lin, L.; Liu, S. J. *Chem Eng J* **2014**, *244*, 137.
- (22) Jimenez-Morales, I.; Moreno-Recio, M.; Santamaria-Gonzalez, J.; Maireles-Torres, P.; Jimenez-Lopez, A. *Appl Catal B-Environ* **2014**, *154*, 190.
- (23) Wang, Z.; Cohen, S. M. *Chem. Soc. Rev.* **2009**, *38*, 1315.
- (24) Furukawa, H.; Cordova, K. E.; O’Keeffe, M.; Yaghi, O. M. *Science* **2013**, *341*.
- (25) Lee, J.; Farha, O. K.; Roberts, J.; Scheidt, K. A.; Nguyen, S. T.; Hupp, J. T. *Chem. Soc. Rev.* **2009**, *38*, 1450.
- (26) Liu, Y.; Xuan, W. M.; Cui, Y. *Adv. Mater.* **2010**, *22*, 4112.

- 
- (27) Ma, L. Q.; Lin, W. B. In *Functional Metal-Organic Frameworks: Gas Storage, Separation and Catalysis*; Schroder, M., Ed.; Springer-Verlag Berlin: Berlin, 2010; Vol. 293, p 175.
- (28) Falkowski, J. M.; Liu, S.; Lin, W. B. *Isr. J. Chem.* **2012**, *52*, 591.
- (29) Doherty, C. M.; Buso, D.; Hill, A. J.; Furukawa, S.; Kitagawa, S.; Falcaro, P. *Accounts Chem. Res.* **2014**, *47*, 396.
- (30) Phan, A.; Doonan, C. J.; Uribe-Romo, F. J.; Knobler, C. B.; O’Keeffe, M.; Yaghi, O. M. *Accounts Chem. Res.* **2009**, *43*, 58.
- (31) Demirci, U. B.; Akdim, O.; Andrieux, J.; Hannauer, J.; Chamoun, R.; Miele, P. *Fuel Cells* **2010**, *10*, 335.
- (32) Wu, R.; Qian, X.; Rui, X.; Liu, H.; Yadian, B.; Zhou, K.; Wei, J.; Yan, Q.; Feng, X. Q.; Long, Y.; Wang, L.; Huang, Y. *Small* **2014**.
- (33) Torad, N. L.; Hu, M.; Ishihara, S.; Sukegawa, H.; Belik, A. A.; Imura, M.; Ariga, K.; Sakka, Y.; Yamauchi, Y. *Small* **2014**.
- (34) Gross, A. F.; Sherman, E.; Vajo, J. J. *Dalton Trans.* **2012**, *41*, 5458.
- (35) Lu, Y. Y.; Zhan, W. W.; He, Y.; Wang, Y. T.; Kong, X. J.; Kuang, Q.; Xie, Z. X.; Zheng, L. S. *ACS Appl. Mater. Interfaces* **2014**, *6*, 4186.
- (36) Yao, J. F.; He, M.; Wang, K.; Chen, R. Z.; Zhong, Z. X.; Wang, H. T. *Crystengcomm* **2013**, *15*, 3601.
- (37) Marceau, E.; Carrier, X.; Che, M. In *Synthesis of Solid Catalysts*; Wiley-VCH Verlag GmbH & Co. KGaA: 2009, p 59.
- (38) Maitra, A. M.; Cant, N. W.; Trimm, D. L. *Applied Catalysis* **1986**, *27*, 9.
- (39) Vincent, R. C.; Merrill, R. P. *Journal of Catalysis* **1974**, *35*, 206.
- (40) Weisz, P. B. *Transactions of the Faraday Society* **1967**, *63*, 1801.
- (41) Weisz, P. B.; Hicks, J. S. *Transactions of the Faraday Society* **1967**, *63*, 1807.
- (42) Harriott, P. *Journal of Catalysis* **1969**, *14*, 43.
- (43) Assaf, E. M.; Jesus, L. C.; Assaf, J. M. *Chem Eng J* **2003**, *94*, 93.
- (44) Goula, M. A.; Kordulis, C.; Lycourghiotis, A. *Journal of Catalysis* **1992**, *133*, 486.
- (45) Li, W. D.; Li, Y. W.; Qin, Z. F.; Chen, S. Y. *Chemical Engineering Science* **1994**, *49*, 4889.
- (46) Papageorgiou, P.; Price, D. M.; Gavriilidis, A.; Varma, A. *Journal of Catalysis* **1996**, *158*, 439.
- (47) Roman-Leshkov, Y.; Barrett, C. J.; Liu, Z. Y.; Dumesic, J. A. *Nature* **2007**, *447*, 982.
- (48) Zu, Y. H.; Yang, P. P.; Wang, J. J.; Liu, X. H.; Ren, J. W.; Lu, G. Z.; Wang, Y. Q. *Appl Catal B-Environ* **2014**, *146*, 244.
- (49) De, S.; Dutta, S.; Saha, B. *Chemsuschem* **2012**, *5*, 1826.

- 
- (50) Binder, J. B.; Raines, R. T. *Journal of the American Chemical Society* **2009**, *131*, 1979.
- (51) Chidambaram, M.; Bell, A. T. *Green Chem* **2010**, *12*, 1253.
- (52) Thananattachon, T.; Rauchfuss, T. B. *Angewandte Chemie* **2010**, *49*, 6616.
- (53) Jae, J.; Zheng, W. Q.; Lobo, R. F.; Vlachos, D. G. *Chemsuschem* **2013**, *6*, 1158.
- (54) Zhang, J.; Lin, L.; Liu, S. *Energy & Fuels* **2012**, *26*, 4560.
- (55) Twigg, M. V.; Spencer, M. S. *Applied Catalysis A: General* **2001**, *212*, 161.
- (56) Nishimura, S.; Ikeda, N.; Ebitani, K. *Catalysis Today* **2013**.
- (57) Huang, Y. B.; Chen, M. Y.; Yan, L.; Guo, Q. X.; Fu, Y. *Chemsuschem* **2014**, *7*, 1068.
- (58) Wang, G. H.; Hilgert, J.; Richter, F. H.; Wang, F.; Bongard, H. J.; Spliethoff, B.; Weidenthaler, C.; Schuth, F. *Nature materials* **2014**, *13*, 293.
- (59) Hansen, T. S.; Barta, K.; Anastas, P. T.; Ford, P. C.; Riisager, A. *Green Chem* **2012**, *14*, 2457.
- (60) Chatterjee, M.; Ishizaka, T.; Kawanami, H. *Green Chem* **2014**, *16*, 1543.
- (61) Ko, C. H.; Park, S. H.; Jeon, J. K.; Suh, D. J.; Jeong, K. E.; Park, Y. K. *Korean J. Chem. Eng.* **2012**, *29*, 1657.
- (62) Karakhanov, E. A.; Maksimov, A. L.; Zolotukhina, A. V.; Kardasheva, Y. S. *Russ. Chem. Bull.* **2013**, *62*, 1465.
- (63) Chen, Q. A.; Ye, Z. S.; Duan, Y.; Zhou, Y. G. *Chem. Soc. Rev.* **2013**, *42*, 497.
- (64) Monguchi, Y.; Sajiki, H. *J. Synth. Org. Chem. Jpn.* **2012**, *70*, 711.
- (65) Rylander, P. *Catalytic Hydrogenation over Platinum Metals*; Elsevier Science, 2012.
- (66) Finley, A. J. *Catalytic Transfer Hydrogenation of Aldehydes and Epoxides Using Raney Nickel and 2-propanol as a Hydrogen Donor*; University of Tennessee at Chattanooga, Chemistry, 2005.
- (67) Roth, P. *Asymmetric Transfer Hydrogenation of Aromatic Ketones and Azirines with NH-ligands*; Acta Universitatis Upsaliensis, 2002.
- (68) Fernandes, V. R.; Pinto, A. M. F. R.; Rangel, C. M. *International Journal of Hydrogen Energy* **2010**, *35*, 9862.
- (69) Kojima, Y.; Suzuki, K.-i.; Fukumoto, K.; Sasaki, M.; Yamamoto, T.; Kawai, Y.; Hayashi, H. *International Journal of Hydrogen Energy* **2002**, *27*, 1029.
- (70) Kim, J.-H.; Lee, H.; Han, S.-C.; Kim, H.-S.; Song, M.-S.; Lee, J.-Y. *International Journal of Hydrogen Energy* **2004**, *29*, 263.
- (71) Wu, C.; Wu, F.; Bai, Y.; Yi, B.; Zhang, H. *Materials Letters* **2005**, *59*, 1748.
- (72) Ye, W.; Zhang, H.; Xu, D.; Ma, L.; Yi, B. *Journal of Power Sources* **2007**, *164*,

544.

(73) Jeong, S. U.; Kim, R. K.; Cho, E. A.; Kim, H. J.; Nam, S. W.; Oh, I. H.; Hong, S. A.; Kim, S. H. *Journal of Power Sources* **2005**, *144*, 129.

(74) Lu, Z.-H.; Yao, Q.; Zhang, Z.; Yang, Y.; Chen, X. *Journal of Nanomaterials* **2014**, *2014*, 1.

(75) Moussa, G.; Moury, R.; Demirci, U. B.; Şener, T.; Miele, P. *International Journal of Energy Research* **2013**, *37*, 825.

(76) Bullock, R. M. *Science* **2013**, *342*, 1054.

